

OWTNM
2019

XXVII International Workshop on
Optical Wave & Waveguide Theory
and Numerical Modelling

Málaga (Spain), May 10-11, 2019

Proceedings

XXVII International Workshop on Optical
Wave & Waveguide Theory and
Numerical Modelling

Málaga, Spain

May 10-11, 2019



OWTNM 2019

XXVII International Workshop on Optical Wave & Waveguide
Theory and Numerical Modelling

Málaga, Spain, May 10-11, 2019

<http://www.owtnm2019.com/>

Proceedings



Esta actividad se realiza con la colaboración del Vicerrectorado con competencias en Investigación y Transferencia de la UMA, del Departamento Ingeniería de Comunicaciones y de la Escuela Técnica Superior de Ingeniería de Telecomunicación de la Universidad de Málaga.

Organizers

Local Steering Committee OWTNM'19

Photonics & RF Research Lab @ Málaga Málaga University
<http://www.photonics-rf.uma.es/>

- Íñigo Molina Fernández (Group leader)
- Alejandro Ortega Moñux
- J. Gonzalo Wangüemert Pérez
- Robert Halir
- José de Oliva Rubio
- Pedro José Reyes Iglesias
- Rafael Godoy Rubio

OWTNM Technical Committee

- Arti Agrawal, City University of London, UK
- Trevor Benson, University of Nottingham, UK
- Jiří Čtyroký, Institute of Photonics and Electronics, Czech Academy of Sciences, Czech Republic
- Anne-Laure Fehrembach, Institut Fresnel, Marseille, France
- Manfred Hammer, Paderborn University, Germany
- Stefan Helfert, FernUniversität Hagen, Germany
- Bastiaan de Hon, Eindhoven University of Technology, The Netherlands
- Andrei Lavrinenko, Technical University of Denmark, Lyngby, Denmark
- Marian Marciniak National Institute of Telecommunications, Warsaw, Poland
- Andrea Melloni, Politecnico di Milano, Italy
- Ivan Richter, Czech Technical University, Prague, Czech Republic
- Dirk Schulz, TU Dortmund University, Germany
- Christoph Wächter, Fraunhofer IOF, Jena, Germany

Preface

The 27th International Workshop on Optical Wave & Waveguide Theory and Numerical Modelling (OWTNM) will be held on May 10th & 11th, 2019 at Málaga University, Málaga, Spain.

The Workshop will be organized in seven oral sessions, where participants from Germany, China, France, Spain, Czech Republic, United Kingdom, India and Greece, will present their latest contributions in the field of theoretical and computational photonics. As usual, a topical collection of the journal Optical and Quantum Electronics will be organized on the occasion of the workshop.

In continuing the friendly spirit that has always been an integral part of the conference, the talks will act as catalyst for the exchange of stimulating ideas during the coffee breaks, lunches, and the social program. This is indeed one of the key points of this Workshop: providing a pleasant environment where attendees can easily find time to discuss their ideas, which is not always easy in large-scale conferences. On the other hand, the city of Málaga provides a fantastic backdrop with pleasant weather, outstanding food and wines, and nice beaches. We hope that attendees will enjoy not only the technical program, but also the life in our beautiful city.

Last but not least important, we, the local organizing committee, want to express our deep gratitude to the invited speakers: Philippe Lalanne, Nicolae C. Panoiu, Jiri Ctyroky, Robert Halir and Carsten Schuck, who will undoubtedly provide exciting perspectives on the frontiers of our field.

Málaga, May 2019.

The local steering committee.

The workshop at a glance

Thursday 9 th	
19:00h	<u>WELCOME RECEPTION</u> <u>“Bodega Bar El Pimpi”, Calle Granada, 62</u>
Friday 10 th	
09.30h - 11.00h	RESONANT STRUCTURES
11:00h - 11:30h	Coffee break
11.30h - 12:30h	PLASMONICS
12:30h - 13:45h	Lunch
13.45h - 15.15h	THEORY AND MODELLING (I)
15:15h - 15:45h	Coffee break
15.45h - 17.00h	THEORY AND MODELLING (II)
19.30h	<u>WORKSHOP DINNER</u> <u>“EL MERENDERO DE ANTONIO MARTÍN”</u> <u>Plaza de la Malagueta 4</u>
Saturday 11 th	
09.30h - 11.00h	GRATINGS
11.00h - 11.30h	Coffee break
11.30h - 12.45h	INTEGRATED PHOTONICS
12.45h - 14.00h	Lunch
14.00h - 14.45h	FIBER OPTICS
14:45h	Closing remarks

Detailed program

Thursday 9 th	
19:00h	<u>WELCOME RECEPTION</u> <u>“Bodega Bar El Pimpi”, Calle Granada, 62</u>

Friday 10 th			
09.30h - 11:00h		RESONANT STRUCTURES	p.1
09:30h - 10:00h	Invited	<i>Ultra-narrowband Bragg filters in subwavelength grating metamaterial waveguides</i> J. Čtyroký, P. Cheben, J. H. Schmid, S. Wang, D. Melati, D. Xu, S. Janz, J. Lapointe, J. G. Wangüemert-Pérez, Í. Molina-Fernández, A. Ortega-Moñux, R. Halir, P. Kwiecien, I. Richter	<i>p. 2</i>
10:00h - 10:15h	Regular	<i>An open rectangular dielectric optical cavity with unlimited Q</i> M. Hammer, L. Ebers, J. Förstner	<i>p. 3</i>
10:15h - 10:45h	Invited	<i>Rigorous modal analysis of photonic micro and nanoresonators</i> P. Lalanne, W. Yan	<i>p. 4</i>
10:45h - 11:00h	Regular	<i>Rigorous Quality Factor Calculation in Contemporary Optical Resonant Systems</i> T. Christopoulos, O. Tsilipakos, G. Sinatkas, E. E. Kriezis	<i>p. 5</i>
11:00h - 11:30h		Coffee break	
11.30h - 12:30h		PLASMONICS	p. 6
11:30h - 11:45h	Regular	<i>Light emission in slow metallic waveguides: overcoming quenching</i> P. Lalanne	<i>p. 7</i>
11:45h - 12:00h	Regular	<i>Design of 3D Si/InSb nonreciprocal waveguiding structures with Magneto optic Rigorous Coupled Wave Analysis</i> P. Kwiecien, I. Richter, V. Kuzmiak, J. Čtyroký	<i>p. 8</i>
12:00h - 12:15h	Regular	<i>Experimental demonstration and numerical study of plasmon-soliton waves</i> G. Renversez, M. M. R. Elsayy, M. Chauvet, T. Kuriakose, T. Halenkovic, V. Nazabal, P. P. Nemec	<i>p. 9</i>
12:15h - 12:30h	Regular	<i>Palladium Grating Assisted Surface Plasmon Resonance Based Hydrogen Sensor</i> A. Bijalwan, B. K. Singh, V. Rastogi	<i>p. 10</i>
12:30h - 13:45h		Lunch	

13.45h - 15.15h		THEORY AND MODELLING (I)	p. 11
13:45h - 14:15h	Invited	<i>Optical Pulse Dynamics in a Silicon Photonic Crystal Waveguide Coupled with a set of Photonic Crystal Optical Cavities</i> V. M. Fernandez Laguna, Q. Ren, and N. C. Panoiu	p. 12
14:15h - 14:30h	Regular	<i>First-order perturbation theory for material changes in the surrounding of open optical resonators</i> S. Both, T. Weiss	p. 13
14:30h - 14:45h	Regular	<i>Photonic crystal slab between orthogonal polarizers: details on the guided mode resonance wavelength</i> H. Lüder, M. Paulsen, M. Gerken	p. 14
14:45h - 15:00h	Regular	<i>Edge states in photonic lattices under periodic driving</i> J. Petráček, V. Kuzmiak	p. 15
15:00h - 15:15h	Regular	<i>Computing Resonant Modes of Circular Cylindrical Structures by Vertical Mode Expansions</i> H. Shi, Y. Y. Lu	p. 16
15:15h - 15:45h		Coffee break	
15.45h – 17.00h		THEORY AND MODELLING (II)	p. 17
15:45h - 16:00h	Regular	<i>Graphene on an optical waveguide - comparison of simulation approaches</i> J. Čtyroký, P. Kwiecien, J. Petráček, V. Kuzmiak, I. Richter	p. 18
16:00h - 16:15h	Regular	<i>Unidirectional vectorial eigenmode propagation for multiscale tapered waveguides in 3D</i> L. Ebers, M. Hammer, J. Philipp Höpker, T. Bartley, J. Förstner	p. 19
16:15h - 16:30h	Regular	<i>Modeling gain in Er3+/Yb3+ co-doped integrated dual-core waveguides</i> D. Benedicto, A. Días, J. A. Vallés, J. C. Martín, J. Solís	p. 20
16:30h - 16:45h	Regular	<i>Design Strategy for a Compact Broadband Directional Coupler Using Adiabatically Tapered Waveguides</i> N. Dhingra, E. K. Sharma	p. 21
16:45h - 17:00h	Regular	<i>Modal Simulation of a Three Lobes Plastic Optical Fiber Bending Sensor</i> D. Sartiano, D. Perez Galacho, F. Berghmans, T. Geernaert, S. Sales	p. 22

19.30h	WORKSHOP DINNER “EL MERENDERO DE ANTONIO MARTÍN” Plaza de la Malagueta 4
---------------	---

Saturday 11 th			
09.30h - 11.00h		GRATINGS	p. 23
09:30h - 10:00h	Invited	Subwavelength grating: from basic physics to state-of-the-art devices R. Halir , A. Sánchez-Postigo, J. M. Luque-González, A. Herrero-Bermello, J. Leuermann, A. Ortega-Moñux, J. G. Wangüemert-Pérez, A. V. Velasco, J. de-Oliva-Rubio, J. H. Schmid, P. Cheben, J. Soler Penadés, M. Nedeljkovic, G. Z. Mashanovich, Í. Molina-Fernández	p. 24
10:00h - 10:15h	Regular	Quasi-total backward reflection with a CRIGF structure under oblique incidence F. Renaud, A. Fehrembach, E. Popov, A. Monmayrant, O. Gauthier-Lafaye	p. 25
10:15h - 10:30h	Regular	Controlling birefringence in silicon photonics SWG waveguides J. M. Luque-González, A. Herrero-Bermello, A. Ortega-Moñux, Í. Molina-Fernández, A. V. Velasco, P. Cheben, J. H. Schmid, S. Wang, R. Halir	p. 26
10:30h - 10:45h	Regular	Fast Fourier Factorization: A Powerful Tool for the Modelling of Non-Lamellar Metallic Gratings Compared to the C-Method H. Mohamad, S. Es-Saidi, A. Morand, P. Benech, D. Macias, S. Blaize	p. 27
10:45h - 11:00h	Regular	Simulation of diffuse scattering due to stochastic disturbances of 1D-gratings M. Heusinger, D. Michaelis, T. Flügel-Paul, U. D. Zeitner	p. 28
11:00h – 11:30h		Coffee break	
11:30h – 12:45h		INTEGRATED PHOTONICS	p. 29
11:30h - 12:00h	Invited	Nanophotonic circuit components for integrated quantum technology C. Schuck	p. 30
12:00h - 12:15h	Regular	Design of a subwavelength grating metamaterial GRIN lens J. M. Luque-González, R. Halir, J. de-Oliva-Rubio, J. G. Wangüemert-Pérez, P. Cheben, J. H. Schmid, Í. Molina-Fernández, A. Ortega-Moñux	p. 31
12:15h - 12:30h	Regular	Simplified modeling of free-carrier based silicon modulators D. Pérez-Galacho, D. Marris-Morini, S. Sales, E. Cassan, C. Baudot, F. Beouf, L. Vivien	p. 32
12:30h - 12:45h	Regular	Efficient Floquet-Bloch analysis of electrically long quasi-periodic devices A. Hadij-ElHouati, P. Cheben, A. Ortega-Moñux, J. G. Wangüemert-Pérez, R. Halir, J. H. Schmid, Í. Molina-Fernández	p. 33
12:45h – 14:00h		Lunch	

14.00h - 14.45h		FIBER OPTICS	p. 34
14:00h - 14:15h	Regular	<i>Splitting of Picosecond Pulses Using Large Mode Area Dispersion Oscillating Fiber at 2.8 μm wavelength</i> M. Rehan, G.Kumar, V. Rastogi	<i>p. 35</i>
14:15h - 14:30h	Regular	<i>Analysis of Fiber Gratings using a Radial Bidirectional Method</i> R. Kumar, A. Sharma	<i>p. 36</i>
14:30h - 14:45h	Regular	<i>Optimization of Device Length in Photonic Lanterns using Shortcuts to Adiabaticity</i> S. Sunder, A. Sharma	<i>p. 37</i>
14:45h		Closing remarks	

Papers

Friday 10 th		
09.30h - 11:00h		RESONANT STRUCTURES
09:30h - 10:00h	Invited	<i>Ultra-narrowband Bragg filters in subwavelength grating metamaterial waveguides</i> J. Čtyroký, P. Cheben, J. H. Schmid, S. Wang, D. Melati, D. Xu, S. Janz, J. Lapointe, J. G. Wangüemert-Pérez, Í. Molina-Fernández, A. Ortega-Moñux, R. Halir, P. Kwiecien, I. Richter
10:00h - 10:15h	Regular	<i>An open rectangular dielectric optical cavity with unlimited Q</i> M. Hammer, L. Ebers, J. Förstner
10:15h - 10:45h	Invited	<i>Rigorous modal analysis of photonic micro and nanoresonators</i> P. Lalanne, W. Yan
10:45h - 11:00h	Regular	<i>Rigorous Quality Factor Calculation in Contemporary Optical Resonant Systems</i> T. Christopoulos, O. Tsilipakos, G. Sinatkas, E. E. Kriezis

Ultra-narrowband Bragg filters in subwavelength grating metamaterial waveguides

Jiří Čtyrský^{1*}, Pavel Cheben², Jens H. Schmid², Shurui Wang², Daniele Melati², Danxia Xu², Siegfried Janz², Jean Lapointe², J. Gonzalo Wangüemert-Pérez³, Íñigo Molina-Fernández³, Alejandro Ortega-Moñux³, Robert Halir³, Pavel Kwiecien⁴, Ivan Richter⁴

¹CAS, Institute of Photonics and Electronics, Prague, Czech Republic,

²National Research Council Canada, Ottawa, Canada

³Universidad de Málaga, Dpto. Ingeniería de Comunicaciones, ETSI Telecomunicación, Málaga, Spain

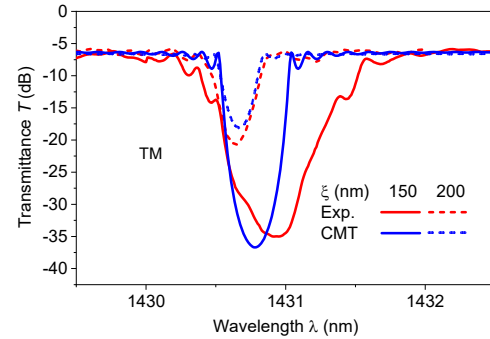
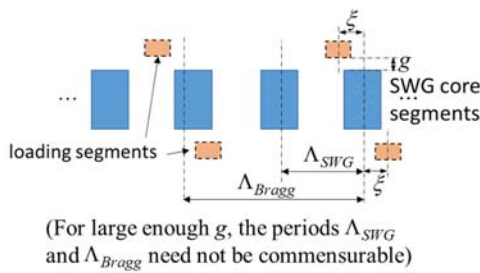
⁴Faculty of Nuclear Sciences and Physical Engineering, Department of Physical Engineering, Czech Technical University in Prague, Prague, Czech Republic

*ctyrosky@ufe.cz

Subwavelength grating (SWG) metamaterial waveguides represent an important platform for silicon photonics [1]. We will describe the design principles of very narrowband Bragg reflection and transmission filters based on SWG waveguides with the minimum feature size as large as 100 nm. We will show that the well-known coupled-mode theory (CMT) is fully applicable to SWG Bragg grating structures [2]. Examples of experimental results will be presented and discussed [3], and a very simple but efficient method for the determination of the sensitivity of Bragg grating filters as refractometric sensors will be demonstrated.

Design of SWG Bragg filters and their properties

To keep the minimum feature size of a very narrowband Bragg grating filters on high-contrast SOI SWG waveguides sufficiently large, we choose the design based on silicon loading segments positioned at a proper distance along both sides of the SWG waveguide (left figure). The coupling constant between the forward and backward (Bloch) modes of the SWG waveguide depends exponentially on the separation g , but can be fine-tuned by the relative longitudinal shift 2ξ of opposite loading segments. Bandwidths of properly designed experimental gratings were found to be as low as 150 pm (right figure). We will also show that the sensitivity of narrow-band Bragg grating used as a refractometric sensor depends predominantly on the effective refractive index of the SWG waveguide and its dispersion, which helps simplify the analysis and design of such sensors.



Configuration of the Bragg grating.

Comparison of measured and simulated transmittances.

References

- [1] P. Cheben, R. Halir, J. H. Schmid, H. A. Atwater, and D. R. Smith, "Subwavelength integrated photonics," *Nature*, vol. 560, pp. 565–572, 2018.
- [2] J. Čtyrský *et al.*, "Design of narrowband Bragg spectral filters in subwavelength grating metamaterial waveguides," *Optics Express*, vol. 26, no. 1, pp. 179-194, 2018.
- [3] P. Cheben *et al.*, "Bragg filter bandwidth engineering in subwavelength grating metamaterial waveguides," *Optics Letters*, vol. 44, no. 4, 1043-1046, 2019.

An open rectangular dielectric optical cavity with unlimited Q

Manfred Hammer*, Lena Ebers, Jens Förstner

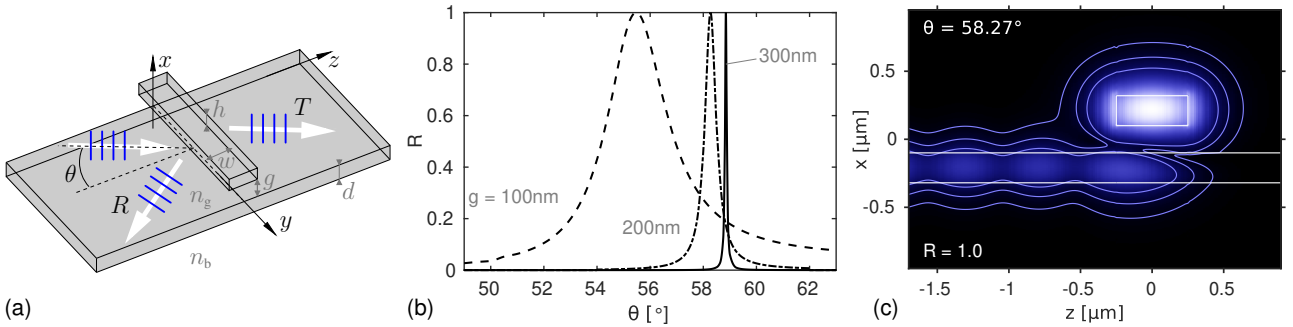
Theoretical Electrical Engineering, Paderborn University, Paderborn, Germany

* manfred.hammer@uni-paderborn.de

Transmission resonances of unlimited quality can be observed in a 2.5-D system where a dielectric strip is excited by semi-guided optical waves at oblique angles of incidence. In a limit of small interaction strength at large gaps between strip and slab, angular and wavelength spectra show fully formed resonances of zero width.

Oblique evanescent excitation of a dielectric strip

Open dielectric optical cavities are always deemed to be inherently lossy. Even in a limit of weak excitation, these inherent losses establish an upper bound to their quality factors (Q-factors). Specifically we look at a dielectric cavity of rectangular shape, such as the resonator device outlined in part (a) of the figure. If considered in a standard 2-D setting, i.e. for normal excitation at angle $\theta = 0$, specific dimensioning of the cavity is required to obtain resonators of tolerable quality. We shall reason in this contribution [1] that the cavity with our — rather arbitrary — parameters supports resonant states of in fact *infinite* Q, in the form of the guided modes of the dielectric strip. Merely a change in excitation conditions is required: We reconsider the resonator device in a “2.5-D” setting, with excitation of the strip by vertically (x -) guided, laterally (y, z -) nonlocalized waves at oblique angles of incidence θ . Radiation losses are suppressed for incidence above a certain critical angle, such that transmittance T and reflectance R total to 100%. Scans (b) over θ then reveal fully formed resonant states (c) with unit reflectance. For growing gap g , the angular width of these resonances decreases, accompanied by an increasing relative intensity in the strip region, while the resonance position approaches the angle associated with the guided mode of the isolated strip. Analogous features can be observed if, for fixed angle of incidence, one varies the frequency of the incoming wave.



Evanescent excitation (a) of a dielectric strip at incidence angle θ . Parameters: $n_g = 3.45$, $n_b = 1.45$, $d = h = 0.22\ \mu\text{m}$, $w = 0.5\ \mu\text{m}$; incoming TE waves at wavelength $\lambda = 1.55\ \mu\text{m}$. (b): Reflectance R versus angle of incidence θ , for varying gaps g ; $R + T = 1$ for $\theta > 46.3^\circ$. (c): Resonance for $g = 200\text{ nm}$, absolute electric field $|E|$ on the x - z -plane.

Bound state coupled to the continuum

In a setting with fixed angle θ and variable frequency, at *large* g , this would be a system with a nonradiating bound state (the rib mode) and a wave continuum (the waves in the slab) in a range of frequencies that cover the eigenfrequency of the bound state. Hence one might argue that this is an explicitly simple way to approach what has been termed a “bound state in the continuum” (BIC).

References

- [1] M. Hammer, L. Ebers, and J. Förstner. Oblique evanescent excitation of a dielectric strip: A model resonator with an open optical cavity of unlimited Q. *Optics Express*, accepted for publication, 2019.

Rigorous modal analysis of photonic micro and nanoresonators

Philippe Lalanne^{1*}, Wei Yan¹

¹ LP2N, Institut d'Optique Graduate School, CNRS, Univ. Bordeaux, 33400 Talence, France

* Philippe.lalanne@institutoptique.fr

The most general motion of a system is a superposition of its normal modes, or eigenstates. We report our recent developments of a rigorous modal analysis of electromagnetic resonators, which is accurate even for geometries that have not been analyzed so far, e.g. 3D resonators made of dispersive media and placed in non-homogeneous backgrounds (on a substrate or an optical thin film stacks).

Modes are central in physics, chemistry ... In optics, modes are self-consistent electromagnetic field distributions in waveguides, optical resonators or in free space (plane waves, Hermite–Gaussian modes ...). In waveguide and free space, they are well documented in the literature, as shown by several textbooks on Fourier optics and optical waveguide theory (Vassalo, Snyder & Love, Marcuse, Collin).

We cannot find any textbook on the modal theory of resonators, although nanoresonances play an essential role in current developments in nanophotonics, e.g., optical metasurfaces, integrated optics, optical sensing, photovoltaic devices... The reason is due to mathematical difficulties, see details in the recent review article [1], and especially to the fact that optical resonators are non-Hermitian systems; their physics is not driven by classical normal modes, but by quasi-normal modes (QNMs) with complex frequencies $\tilde{\omega}$. Presently, about 10 groups in the world are developing a modal theory for analyzing light scattering by resonators.

At the conference, we will present our main recent achievements that can be found in [2] :

- Of particular importance in our work is the successful generalization of the auxiliary-field method, originally proposed for simulating dispersive media with finite difference time-domain simulations [3], to successfully implement a QNM solver that efficiently computes the eigenstates of plasmonic resonators with finite element methods (FEMs). The achieved precision is high, especially for the usual cases of metallic nanoresonators with curved shapes. The QNM solver is implemented in a COMSOL Multiphysics computational platform that can be downloaded at [4].
- On the theoretical side, another important consequence of the auxiliary-field method is a net physical interpretation of temporal dispersion, which lead us to derive orthogonality relations in the augmented formulation for resonances made of dispersive media. Such a derivation that was not possible in earlier works with unspecified dispersion relation [1] leads to the important proposition of closed-form expressions for the eigenstate excitation coefficients.

References

- [1] P. Lalanne, W. Yan, V. Kevin, C. Sauvan, and J.-P. Hugonin, *Light interaction with photonic and plasmonic resonances*, Laser & Photonics Reviews **12**, 1700113 (2018).
- [2] W. Yan, R. Faggiani, and P. Lalanne, *Rigorous modal analysis of plasmonic resonators*, Phys. Rev. B **97**, 205422 (2018)
- [3] R. M. Joseph, S. C. Hagness and A. Taflove, *Direct time integration of Maxwell's equations in linear dispersive media with absorption for scattering and propagation of femtosecond electromagnetic pulses*, Opt. Lett. **16**, 1412 (1991).
- [4] <https://www.lp2n.institutoptique.fr/Membres-Services/Responsables-d-equipe/LALANNE-Philippe>

Rigorous Quality Factor Calculation in Contemporary Optical Resonant Systems

Thomas Christopoulos^{1,*}, Odysseas Tsilipakos², Georgios Sinatkas¹, Emmanouil E. Kriezis¹

¹ School of Electrical & Computer Engineering, AUTH, Thessaloniki 54124, Greece

² Institute of Electronic Structure & Laser, FORTH, Heraklion 71110, Crete, Greece

* cthomasa@ece.auth.gr

Accurate approaches on calculating the quality factor of contemporary optical resonant systems, involving dispersive dielectrics, metals, and 2D materials, are systematically presented. Such resonant systems exhibit high material dispersion and important ohmic and/or radiation losses, rendering typical Q -factor calculation methods, roughly accurate in conventional dielectric resonators, principally erroneous.

Q -factor calculation techniques

The quality factor Q , a measure of the overall cavity loss, specifies the spectral bandwidth, the energy decay rate, and the possible enhancement of a nonlinear resonator's response [1]. Thus, its correct calculation is of outmost importance, being extensively used in linear and nonlinear temporal coupled-mode theory (CMT) frameworks [2] to easily assess resonators' complex response without resorting to cumbersome full-wave simulations.

Here, we collectively present the available methods on calculating the quality factor of nanophotonic resonant systems, computationally simulated using commercially available frequency-domain finite-element method (FEM) software. Specifically, we present the correct approaches to calculate Q using either eigenvalue or time-harmonic simulations, employing: (i) the complex eigenfrequency, (ii) the complex eigenmode, (iii) the actual field spatial distribution, or (iv) the resonator's spectral response. Although well established for conventional dielectric resonators [Fig. 1(a)], the four above techniques should be carefully applied to contemporary nanophotonic resonant systems, such as graphene-comprising resonators, dielectric metasurfaces, and plasmonic nanoparticles [Figs. 1(b)-(d)], to correctly account for the material dispersion, ohmic loss, and light leakage effects. We systematically discuss on the appropriate modifications that should be introduced for the correct Q -factor calculation and demonstrate a remarkable, almost 100% error when applying conventional methods to highly dispersive systems (graphene tubes, plasmonic nanoparticles, etc.). Furthermore, the applicability limits of each modified approach are consistently highlighted.

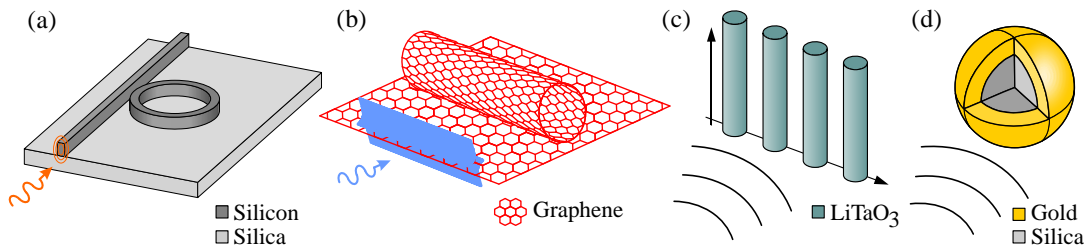


Fig. 1 Optical resonant systems: (a) Silicon microring resonator, (b) graphene tube resonator, (c) dielectric rod metasurface, and (d) plasmonic core-shell nanoparticle.

Acknowledgement

This research was co-financed by Greece and the European Union (ESF) through the Operational Program “Human Resources Development, Education and Lifelong Learning 2014-2020” in the context of the project “Nonlinear phenomena in graphene-comprising resonators” (MIS 5004717).

References

- [1] M. Soljačić and J. D. Joannopoulos, *Nat. Mater.* **3**(4), 211, 2004
- [2] O. Tsilipakos, T. Christopoulos, and E. E. Kriezis, *J. Lightw. Technol.* **34**(4), 1333, 2016

Computing Resonant Modes of Circular Cylindrical Structures by Vertical Mode Expansions

Hualiang Shi¹, Ya Yan Lu²

¹ School of Science, Hangzhou Dianzi University, Hangzhou, China

² Department of Mathematics, City University of Hong Kong, Hong Kong
mayylu@cityu.edu.hk

A vertical mode expansion method is developed to calculate resonant modes of open circular cylindrical structures. The complex frequency of a resonant mode is solved from a carefully designed equation that works well even when the associated matrix is ill-conditioned. The method is used to find subwavelength dielectric cylinders with high Q resonances.

Background

Circular cylindrical resonators or cavities appear frequently in plasmonics, metasurfaces and other nanophotonics applications. Despite its simple geometry, resonant modes of a circular cylinder (of finite height, surrounded by air or placed on a substrate) can only be solved numerically. Correct numerical solutions have appeared in the early 1980's, but accurate numerical solutions are still difficult to find. Due to the field singularity at the edges, most numerical methods converge slowly.

Method and results

For a (possibly layered) circular cylinder embedded in a (possibly layered) background, the vertical mode expansion method (VMEM) [1] based on 1D vertical modes (functions of z , where z is the axis of the cylinder) and horizontal analytic solutions (Bessel and Hankel functions in radial variable r), is very natural and easy to implement. For scattering problems, VMEM gives a linear system $\mathbf{A}\mathbf{x} = \mathbf{c}$, where \mathbf{x} is a vector for the expansion coefficients, \mathbf{c} is related to the incident wave, and \mathbf{A} depends on frequency ω . To find a resonant mode, we determine a complex ω , such that $\mathbf{A}(\omega)$ is singular. The matrix \mathbf{A} maybe be ill-conditioned (i.e., near singular) even when ω is not close to a complex resonant frequency. In that case, it is difficult to find the resonant frequencies using the determinant or the smallest singular (or eigenvalue) of \mathbf{A} . Our approach is to choose vectors \mathbf{c} and \mathbf{b} , and solve ω from $f(\omega) = 1/(\mathbf{b}^T \mathbf{A}^{-1} \mathbf{c}) = 0$. The vector \mathbf{c} is chosen, so that the scattering solution \mathbf{x} has a significant overlap with the desired resonant mode, and \mathbf{b} is chosen from the columns of the identity matrix to select a particular vertical mode which is important for expanding the resonant mode. With this strategy, we are able to determine the resonant modes to high accuracy without the trouble of ill-conditioning.

As an example, we calculate resonant modes with high Q -factors for subwavelength dielectric cylinders [2]. For a cylinder (in air) with dielectric constant 10.73 and radius-height ratio 0.7, we found a resonant mode with normalized frequency $\omega R/(2\pi c) = 0.28724 - 0.001275i$, where R is the radius. The Q factor of this mode is 113, while the Q factors of the other modes are only about 10.

References

- [1] X. Lu and Y. Y. Lu, *Analyzing bull's eye structures by a vertical mode expansion method with rotational symmetry*, J. Opt. Soc. Am. B **32**, 2294-2298 (2015).
- [2] L. Carletti, K. Koshelev, C. De Angelis, and Y. Kivshar, *Giant nonlinear response at the nanoscale driven by bound states in the continuum*, Phys. Rev. Lett. **121**, 033903 (2018).

Friday 10 th		
11.30h - 12.30h	PLASMONICS	
11:30h - 11:45h	Regular	<i>Light emission in slow metallic waveguides: overcoming quenching</i> P. Lalanne
11:45h - 12:00h	Regular	<i>Design of 3D Si/InSb nonreciprocal waveguiding structures with Magneto-optic Rigorous Coupled Wave Analysis</i> P. Kwiecien, I. Richter, V. Kuzmiak, J. Čtyroký
12:00h - 12:15h	Regular	<i>Experimental demonstration and numerical study of plasmon-soliton waves</i> G. Renversez, M. M. R. Elsayy, M. Chauvet, T. Kuriakose, T. Halenkovic, V. Nazabal, P. P. Nemec
12:15h - 12:30h	Regular	<i>Palladium Grating Assisted Surface Plasmon Resonance Based Hydrogen Sensor</i> A. Bijalwan, B. K. Singh, V. Rastogi

Light emission in slow metallic waveguides: overcoming quenching

Philippe Lalanne*

LP2N, Institut d'Optique Graduate School, CNRS, Univ. Bordeaux, 33400 Talence, France

* Philippe.lalanne@institutoptique.fr

Very large spontaneous-emission-rate enhancements (~ 1000) are obtained for quantum emitters coupled with tiny plasmonic resonance, especially when emitters are placed in the mouth of nanogaps formed by metal nanoparticles that are nearly in contact. This fundamental effect of light emission at subwavelength scales is well documented and understood as resulting from the smallness of nanogap modes. In contrast, it is much less obvious to figure out whether the radiation efficiency is high in these gaps, or if the emission is quenched by metal absorption especially for tiny gaps a few nanometers wide; the whole literature only contains scattered electromagnetic calculations on the subject, which suggest that absorption and quenching can be kept at a small level despite the emitter proximity to metal. Thus, through analytical derivations in the limit of small gap thickness, it is our objective to clarify why quantum emitters in nanogap antennas offer good efficiencies, what are the circumstances in which high efficiency is obtained, and whether there exists an upper bound for the maximum efficiency achievable.

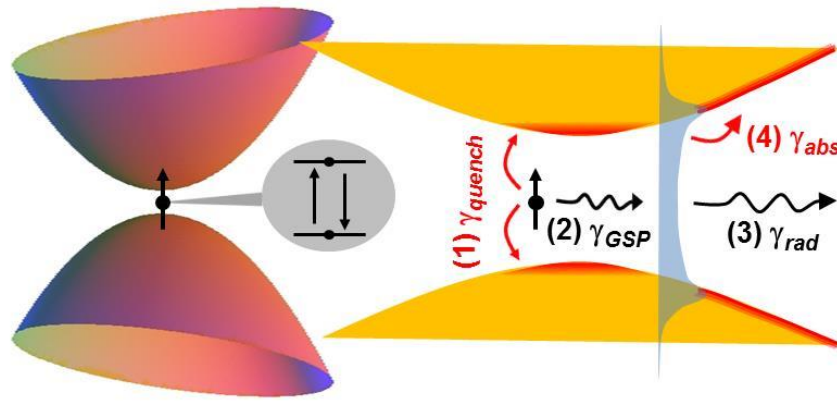


Figure 1. Schematics for understanding modified emission in tiny gaps. (1) Near-field non-radiative decay (quenching) at rate γ_{quench} of the emitter into the metal; (2) Excitation of gap plasmons at rate γ_{GSP} ; (3) Conversion of the excited plasmons into free space photons at rate γ_{gap} ; (4) Plasmon decay into metal at rate γ_{abs} . The quantum emitter is assumed to have an 100% internal quantum efficiency.

References

- [1] P. Lalanne et al., *Structural Slow Waves: Parallels between Photonic Crystals and Plasmonic Waveguides*, ACS Photonics **6**, 4-17 (2019).

Design of 3D Si/InSb nonreciprocal waveguiding structures with Magneto-optic Rigorous Coupled Wave Analysis

P. Kwiecien¹, I. Richter^{1*}, V. Kuzmiak,² J. Čtyroký²

¹ Czech Technical University in Prague, Faculty of Nuclear Sciences and Physical Engineering, Department of Physical Electronics, Břehová 7, 11519 Prague 1, Czech Republic

² CAS Institute of Photonics and Electronics, Chaberská 57, 182 51 Praha 8, Czech Republic

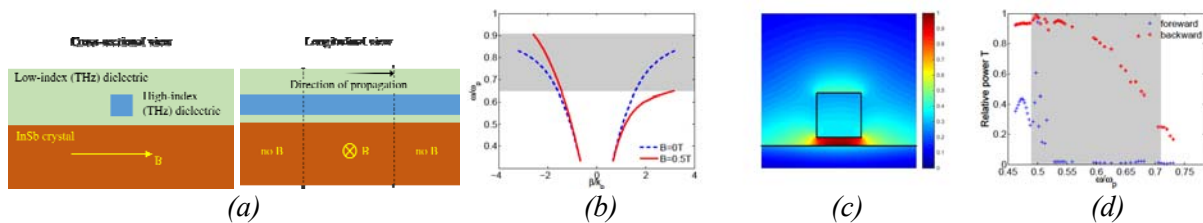
* ivan.richter@fjfi.cvut.cz

One of only few possibilities how to impose nonreciprocity in guiding subwavelength structures is to apply an external magnetic field (mainly in the Voigt configuration). In such a case, one-way (nonreciprocal) propagation of surface plasmons is not only possible but may bring many interesting phenomena in connection with magnetoplasmons (MSP). Based on our 3D Magneto-optic aperiodic Fourier modal method (MOaRCWA), we have studied such THz magnetoplasmons in a combined 3D MO structure, based on a combination of the 2D highly-dispersive polaritonic InSb-based MO structure and 3D hybrid Si-based plasmonic slot waveguide structure, operating at the THz range. The obtained results will be discussed and the perspective will be given.

3D nonreciprocal Si/InSb hybrid dielectric-plasmonic slot waveguide structure

We have developed an efficient 3D numerical technique based on fully anisotropic aperiodic rigorous coupled wave analysis and applied it for simulating magnetoplasmonic nonreciprocal structures (MOaRCWA [1,2]). In our in-house tool, the artificial periodicity is imposed within a periodic 2D RCWA method, in the form of the complex transformation and / or uniaxial perfectly matched layers, thus enabling the simulation of fully 3D structures. Using this technique, we have designed a novel hybrid THz range structure, based on 2D polaritonic InSb-based MO structure and a 3D hybrid Si-based plasmonic slot waveguide. As an example, Fig show the structure studied in both cross-sectional and longitudinal views (a), the dispersion reciprocal ($B = 0$ T) and nonreciprocal ($B = 0.5$ T) band diagrams indicating the one-way band gap $[0.65, 0.906]\omega/\omega_p$ (b). Also, mode intensity profile for $B=0.5$ T and $\lambda_p=300$ μm is presented (c), together with the relative forward and backward spectral transmittances ($L=300$ μm) for the case when losses were not taken into account (d) the one-way band gap is shown in grey color. We have shown that the one-way bandwidth can be controlled by an external magnetic field. Based on such analysis of simple guiding structures, one could consider more complex MO InSb microstructures in THz range.

Acknowledgements: This work was financially supported by the Czech Science Foundation (project 19-00062S).



(a) Schematic of the 3D MO Si/InSb structure - cross-sectional and longitudinal views, (b) dispersion nonreciprocal band diagram $B=0.5$ T, gap $[0.65, 0.906]\omega/\omega_p$, (c) mode intensity profile, $B=0.5$ T, $\lambda_p=300$ μm , (d) relative forward and backward spectral transmittances for $L=300$ μm (without losses). The one-way band gap is shown in grey color.

- [1] P. Kwiecien, I. Richter, V. Kuzmiak, J. Čtyroký, "Nonreciprocal waveguiding structures for THz region based on InSb," JOSA A 34 (6), 892 (2017).
- [2] P. Kwiecien, I. Richter, V. Kuzmiak, J. Čtyroký, "Nonreciprocal MO Waveguiding Structures Studied with Magneto-optic Rigorous Coupled Wave Analysis," Photonics West 2019, [10921-54] (2019).

Experimental demonstration and numerical study of plasmon-soliton waves

Gilles Renversez^{1,*}, Mahmoud M. R. Elsaywy¹, Mathieu Chauvet², Tintu Kuriakose², Tomaz Halenkovic³, Virginie Nazabal⁴, Petr P. Němec³,

¹ Aix-Marseille Univ, CNRS, Centrale Marseille, Institut Fresnel, Marseille, 13013, France

² FEMTO-ST Institute, CNRS, Université de Bourgogne Franche-Comté, 25030 Besançon, France

³ Faculty of Chemical Technology, University of Pardubice, 53210 Pardubice, Czech Republic

⁴ Institut des sciences chimiques de Rennes, CNRS, Université de Rennes 1, 35042 Rennes, France

*gilles.renversez@univ-amu.fr

We present the first experimental observation of plasmon-soliton waves. The indirect demonstration is performed in a chalcogenide-based multilayered planar waveguide with gold structures that exhibits an efficient Kerr self-focusing at moderate power. We also provide a detailed numerical study of the phenomenon.

Merging the fields of plasmonics and nonlinear optics authorizes a variety of fascinating and original physical phenomena. In this work, we specifically study the combination of the strong light confinement ability of surface plasmon polaritons (SPP) with the beam self-trapping effect in a nonlinear optical Kerr medium. Although this idea of plasmon-soliton has been the subject of numerous theoretical papers since the eighties [1-4], up to now, no experimental evidence had been revealed yet. In the present study, a proper structure has been first designed and then fabricated allowing the first experimental demonstration of these hybrid nonlinear waves merging spatial solitons and SPP. To be able to trigger the nonlinearity at moderate light power and simultaneously to allow propagation over several millimeters, a multilayered dielectric-metal structure was first designed by nonlinear FEM modeling [5]. It consists of a five-layer planar geometry made from a silicon wafer with a thick silica layer covered by a chalcogenide layer that is covered with a 10 nm silica layer followed by a gold film. Performed numerical simulations show that the main nonlinear TM modes of the designed planar waveguide exhibits a strongly enhanced Kerr self-focusing thanks to the plasmonic effect compared to the main TE nonlinear mode. The experimental analysis consists in injecting a typical $4 \times 30 \mu\text{m}^2$ (FWHM) elliptical beam at $1.55 \mu\text{m}$ from a femtosecond laser into the 5 mm long structure. The output beam distribution evolution is then monitored versus input light intensity. It shows that a large trapping enhancement is observed for a TM mode in presence of the plasmonic structure compared to configurations where the plasmonic effect is absent. For an input intensity of 1.17 GW/cm^2 the beam is self-confined to a $12 \mu\text{m}$ FWHM while the FWHM is twice larger without plasmonic effect. Our plasmonic structure definitely exposes an enhanced self-focusing nonlinearity. The strong light confinement is due to the presence of the plasmon-soliton wave that propagates in the structures only for the TM polarization. Different configurations have been characterized, and they have been modeled using an improved version of the spatial NLSE to study the propagation in the full structure [6].

References

- [1] V. M. Agranovich, V. Babichenko, *et al.*, "Nonlinear surface polaritons," JETP Lett 32, p. 512 (1980).
- [2] J. Ariyasu, C. T. Seaton, G. I. Stegeman, A. A. Maradudin, and R. F. Wallis, "Nonlinear surface polaritons guided by metal films," J. Appl. Phys. 58, p. 2460 (1985).
- [3] E. Feigenbaum and M. Orenstein, "Plasmon soliton," Opt. Lett. 32(6), p. 674 (2007).
- [4] W. Walasik, V. Nazabal, M. Chauvet, Y. Kartashov, and G. Renversez, "Low-power plasmon-soliton in realistic nonlinear planar structures," Opt. Lett. 37(22), p. 4579 (2012).
- [5] M. M. R. Elsaywy and G. Renversez, "Exact calculation of the nonlinear characteristics of 2D isotropic and anisotropic waveguides", Opt. Lett., vol. 43(11), p. 2446, (2018).
- [6] T. Kuriakose, G. Renversez, V. Nazabal, M. Elsaywy, T. Halenkovic, P. Němec, and M. Chauvet, "Experimental demonstration of plasmon-soliton coupling", arXiv:1811.06525 [physics.optics], (2018).

Palladium Grating Assisted Surface Plasmon Resonance Based Hydrogen Sensor

Ashish Bijalwan*, Bipin K Singh, Vipul Rastogi

Department of Physics, Indian Institute of Technology Roorkee, Uttarakhand, India

*ashis.dph2014@iitr.ac.in, bipinsngh312@gmail.com, vipulph@iitr.ac.in

We present a hydrogen sensor based on Pd-grating/Au/Al layered structure. Sandwiched Au layer acts as a protective layer and provides chemical stability to the sensor. Numerical simulations show that the proposed hydrogen sensor has better sensing characteristics than those of conventional Pd grating based sensor.

Hydrogen, an alternate to fossil fuel, is widely used in many industries like power sectors, petroleum processing, and metallurgical application. In spite of several advantages, hydrogen is explosive and extremely flammable. Therefore, the utilization of hydrogen is potentially hazardous. To reduce the risk associated with it, highly sensitive and reliable sensors are required. Several hydrogen sensors have been developed based on different principles and among those SPR sensors have attracted much research interest [1]. In this paper, we present an SPR based hydrogen sensor by using Pd grating over Al film. To prevent the oxidation of Al we propose to use an ultrathin Au layer in between Pd grating and Al film. The schematic of the sensor is shown in Fig. 1 (a). Palladium is the best candidate for the detection of hydrogen. When Pd comes in contact with hydrogen, it absorbs hydrogen and forms PdH_x (x is the atomic ratio of H/Pd). Absorption of hydrogen results in a reduction of the permittivity of Pd, which expressed as [2]:

$$\varepsilon_{\text{Pd},c\%H_2} = h(c) \times \varepsilon_{\text{Pd},0\%H_2}$$

where $\varepsilon_{\text{Pd},c\%H_2}$ is the complex permittivity of the Palladium layer in absence of hydrogen gas, whereas $\varepsilon_{\text{Pd},0\%H_2}$ is its dielectric function in presence of hydrogen gas. This change in the permittivity of Pd is the key for the detection of the concentration of hydrogen. SPR response of the sensor is very sensitive to the optical properties of metal and shifts due to the change of the permittivity of Pd. To study the performance of the sensor, numerical simulations based on RCWA have been carried out [3].

SPR responses of the proposed sensor for 0 and 4% concentration of hydrogen are shown in Fig. 1 (b). We observe that SPR curve shifts toward smaller angle as the concentration of hydrogen increases. 4% concentration is the lower limit of explosion and the sensor studied here is capable enough to sense this much lower concentration of hydrogen. Our study shows that the insertion of Au layer makes the sensor more stable without much affecting the performance of the sensor.

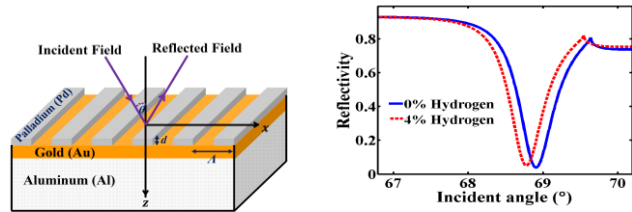


Fig. 1. (a) Schematic of the sensor, and (b) SPR response of the sensor for 0 and 4% of hydrogen concentration.

References

- [1] J. Shao, W. Xie, X. Song, and Y. Zhang, "A new hydrogen sensor based on SNS fiber interferometer with Pd/WO_3 coating," *Sensors*, **17**, 2144, (2017).
- [2] P. Tobiška, O. Hugon, A. Trouillet, and H. Gagnaire, *An integrated optic hydrogen sensor based on SPR on palladium*, *Sens. Actuators B: Chem.*, **74**, 168-172 (2001).
- [3] M. G. Moharam, E. B. Grann, D. A. Pommet, and T. K. Gaylord, *Formulation for stable and efficient implementation of the rigorous coupled-wave analysis of binary gratings*, *J. Opt. Soc. Am. A*, **12**, 1068-1076 (1995).

Friday 10 th		
13.45h - 15.15h	THEORY AND MODELLING (I)	
13:45h - 14:15h	Invited	<i>Optical Pulse Dynamics in a Silicon Photonic Crystal Waveguide Coupled with a set of Photonic Crystal Optical Cavities</i> V. M. Fernandez Laguna, Q. Ren, and N. C. Panoiu
14:15h - 14:30h	Regular	<i>First-order perturbation theory for material changes in the surrounding of open optical resonators</i> S. Both, T. Weiss
14:30h - 14:45h	Regular	<i>Photonic crystal slab between orthogonal polarizers: details on the guided mode resonance wavelength</i> H. Lüder, M. Paulsen, M. Gerken
14:45h - 15:00h	Regular	<i>Edge states in photonic lattices under periodic driving</i> J. Petráček, V. Kuzmiak
15:00h - 15:15h	Regular	<i>Computing Resonant Modes of Circular Cylindrical Structures by Vertical Mode Expansions</i> H. Shi, Y. Y. Lu

Optical Pulse Dynamics in a Silicon Photonic Crystal Waveguide Coupled with a set of Photonic Crystal Optical Cavities

Victor Manuel Fernandez Laguna, Qun Ren, and Nicolae C. Panoiu*

*Department of Electronic and Electrical Engineering, University College London, Torrington Place,
London, UK*

* n.panoiu@ucl.ac.uk

We introduce a rigorous theoretical model that describes the propagation of optical pulses in silicon photonic crystal waveguides and their interaction with photonic crystal cavities and employ it to investigate nonlinear optical effects such as pulse compression, self-phase modulation, and slow-light enhancement of nonlinear optical interactions.

In this paper, we introduce a comprehensive and rigorous theoretical model for pulse propagation in coupled silicon photonic crystal cavity-waveguide nanostructures, along with its computational implementation. The mathematical model, which is based on the coupled-mode theory, takes into account the cavity-waveguide coupling effects, key nonlinear interactions such as the Kerr effect, two-photon-absorption, free-carrier (FC) dispersion and FC absorption, as well as waveguide dispersion effects.

We also discuss how the set of coupled nonlinear Schrödinger equations describing the pulse dynamics is solved numerically using the Newton-Raphson technique for nonlinear systems of partial differential equations and how the key input parameters are calculated using the field profiles of the photonic crystal cavity modes and photonic crystal waveguide modes, which are obtained by numerically solving the Maxwell equations.

The theoretical model and computational method are then employed to analyze the propagation of optical pulses in a photonic system consisting of two interacting photonic crystal cavities coupled to a photonic crystal waveguide operating in the slow-light regime. In particular, we solve the pulse dynamics of forward- and backward-propagating pulses, both in time and frequency domains; the time dependence of the energy contained in each cavity; and the FC dynamics in the cavities and waveguide. Moreover, the influence of different system parameters, such as the separation between cavities, the distance between the cavities and the waveguide, and the width of the input pulse, on the photonic system characteristics is investigated, too. In particular, we illustrate how the theoretical and computational tools can be employed to find the optimum separation between cavities that minimizes the amplitude of the backward-propagating pulse at the input port.

First-order perturbation theory for material changes in the surrounding of open optical resonators

Steffen Both ^{1,*} and Thomas Weiss ¹

¹ *4th Physics Institute and Research Center SCoPE, University of Stuttgart, Germany*

**s.both@pi4.uni-stuttgart.de*

We present a first-order perturbation theory to predict resonance shifts and linewidth changes under small variations of the surrounding materials in almost any kind of open optical resonator. Our method allows to drastically reduce computational efforts and has potential applications for sensor designs.

In recent years, nanophotonics has emerged to a powerful platform for various kinds of optical sensing applications. The typical operation principle is the following: Changes in the local environment of an open optical resonator lead to shifts of its resonance frequencies, and these shifts are then detected optically [1]. Examples for open resonators are plasmonic nanoantennas, dielectric nanoparticles, as well as photonic crystals.

In order to design and optimize such systems with regard to their sensing capabilities, theoretical modeling becomes important. Usually this relies on full numerical simulations, which, however, have the disadvantage that they can be very time consuming, since, in order to calculate the response of the sensor to variations of the analyte substances, the simulations have to be repeated many times.

A way to drastically reduces the computational effort consists in perturbative theories. Such theories are based on the eigenmodes of the system, also known as resonant states or quasi-normal modes. The idea is the following: once the eigenmodes of the unperturbed system are known, e.g., from a single simulations, the influence of perturbations to the system can be calculated analytically without relying on repetitive simulations. Such theories have been proven to be very efficient for describing all kinds of changes within or in close proximity to open optical resonators. Based on existing works [1, 2], we recently have developed a way to also account for changes within the surrounding of the resonator. Our main result is a simple integral expression over the fields of the unperturbed system, that, in first-order approximation, directly provides the resonance shift and linewidth change as a function of the perturbation. We discuss the basic concept of our approach and apply it to two example systems, one from the field of plasmonics and one from the field of photonic crystals.

References

- [1] T. Weiss, M. Mesch, M. Schäferling, H. Giessen, W. Langbein, and E. A. Muljarov, “From Dark to Bright: First-Order Perturbation Theory with Analytical Mode Normalization for Plasmonic Nanoantenna Arrays Applied to Refractive Index Sensing,” *Phys. Rev. Lett.* **116**, 237,401 (2016).
- [2] J. Yang, H. Giessen, and P. Lalanne, “Simple Analytical Expression for the Peak-Frequency Shifts of Plasmonic Resonances for Sensing,” *Nano Letters* **15**(5), 3439–3444 (2015).

Photonic crystal slab between orthogonal polarizers: details on the guided mode resonance wavelength

Hannes Lüder*, Moritz Paulsen, Martina Gerken

Chair for Integrated Systems and Photonics, Faculty of Engineering, Kiel University, Germany

*halu@tf.uni-kiel.de

The transmission spectrum of a photonic crystal slab features sharp dips created by guided mode resonances. The same photonic crystal slab placed between orthogonal polarizers shows peaks at the guided mode resonances. We analyse the wavelength difference between the dips and the peaks.

When a photonic crystal slab (PCS) is placed between two orthogonal polarization filters (Fig. (a)), the total transmission spectrum shows maxima at the guided-mode resonances on a nearly zero background transmission signal, while the photonic crystal slab alone exhibits sharp dips on a high background transmission signal [1]. A wavelength difference $\Delta\lambda = |\lambda_{\text{peak}} - \lambda_{\text{dip}}| = 5.7 \text{ nm}$ is predicted with finite-difference time-domain (FDTD) simulations for a Nb_2O_5 photonic crystal slab with a period of 350 nm, a grating depth of 60 nm and a thickness of 85 nm on a glass substrate. Experimentally, $\Delta\lambda \approx 5 \text{ nm}$ is found.

We present a consistent and easy-understandable explanation for the wavelength difference (shown in Fig. (b)) based on the amplitudes and phases of the transmitted TE and TM polarized waves, which we calculate using temporal coupled-mode theory [2]. For this calculation, we use the simplified model structure shown in Fig. (a). The wavelength difference stems from the Fano asymmetry, but can also be intuitively explained by analysing the transmitted field's polarization state (Fig. (c)).

We also show how this explanation relates to finite-difference time-domain pulse simulations [3] and finite-element Bloch-mode calculations and compare simulation results with measurements.

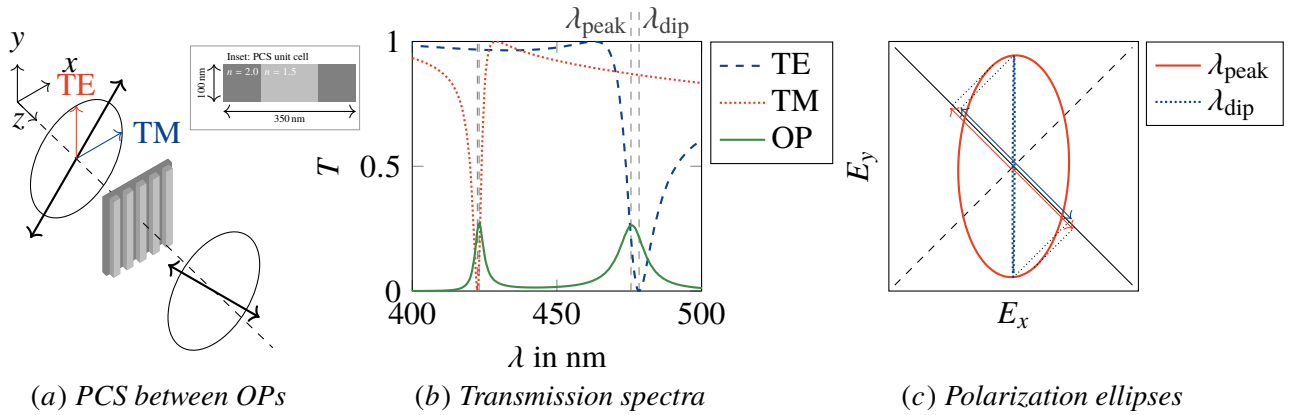


Figure. (a) Photonic crystal slab placed between orthogonal polarizers. The electric field orientations for E_{TE} and E_{TM} are indicated. Inset: unit cell of the analysed photonic crystal slab. (b) Transmission spectra of a PCS for TE and TM polarized light and for the orthogonal polarizer (OP) setup. (c) Polarization ellipses for wavelengths λ_{peak} and λ_{dip} . The projection onto the second polarizer's orientation (solid black diagonal) is indicated. Due to the elliptical polarization, the projected field is slightly larger at λ_{peak} than at λ_{dip} .

References

- [1] Y. Nazirizadeh et. al, Opt. Express 16, 7153-7160 (2008).
- [2] S. Fan, W. Suh, and J. D. Joannopoulos, J. Opt. Soc. Am. A 20, 569-572 (2003).
- [3] S. Fan, J. D. Joannopoulos, Phys. Rev. B 65.23, 235112 (2002).

The authors acknowledge support by Interreg (Project Rollflex, 1_11.12.2014).

Edge states in photonic lattices under periodic driving

Jiří Petráček^{1,*}, Vladimír Kuzmiak²

¹ Brno University of Technology, Institute of Physical Engineering, Brno, Czech Republic

² Czech Academy of Sciences, Institute of Photonics and Electronics, Prague, Czech Republic

*petracek@fme.vutbr.cz

We use a photonic implementation of the topological Su-Schrieffer-Heeger (SSH) model and address the question how time-periodic perturbations affect the topological edge states.

Results

The time-dependent driving can be simulated in the waveguide model consisting of one-dimensional photonic lattice of identical single-mode waveguides (placed along z direction) with space-periodic (in z) modulation of coupling coefficients. By using Floquet theory we study the spectral and topological properties of the system. In particular, we are interested in the population of newly created edge states at the topological transitions in Floquet spectra at which the topology of the system becomes trivial or nontrivial and vice versa. By inspecting the population of the quasi energy spectrum we discuss the difference in nature of the new states.

Results of Floquet analysis are confirmed by numerical simulations. For example, the left panel of Fig. 1 shows spectra of finite systems with 100 waveguides and alternating coupling coefficients $C_{1,2} = C_0 \mp \Delta C \pm \Delta V \sin(\omega z)$, where $\Delta C/C_0 = 0.3$ [1] and $\Delta V/C_0 = 0.4$. We excited the 1st waveguide at $z = 0$ and calculated power remaining in (possibly excited) edge mode(s). The results correspond with quasi energy band diagrams which account for low, intermediate and high frequency ranges [1]. Remarkably, the spectra shown in Fig. 1 associated with trivial and nontrivial phase resemble to some extent complementarity in the annihilation and creation of the edge states in both phases in the SSH model, where driving in nontrivial phase annihilates the topological edge states present in the undriven system while it may create new edge states in the trivial phase as illustrated in the right panel of Fig. 1.

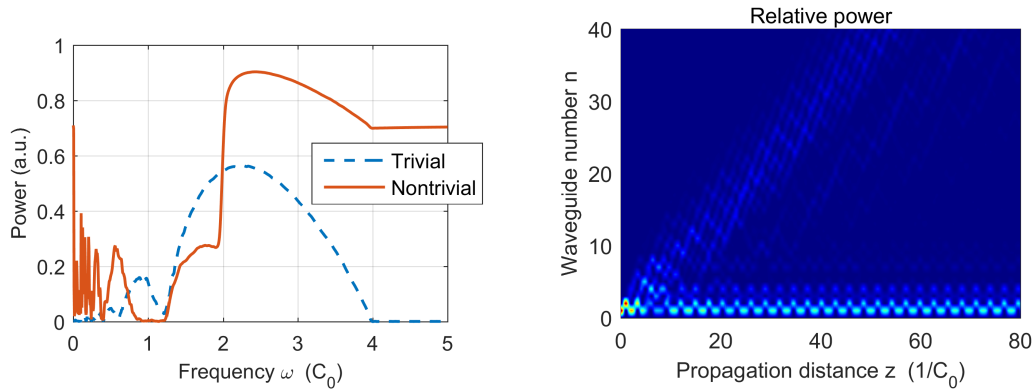


Fig. 1. Left panel: Power coupled into edge states vs. driving frequency ω for trivial and nontrivial phase. Right panel: Excitation of edge states in trivial phase at $\omega/C_0 = 2.23$.

References

- [1] V. Dal Lago, M. Atala, and L. E. F. Foa Torres, *Floquet topological transitions in a driven one-dimensional topological insulator*, Phys. Rev. A, Vol. 92, No. 2, 023624, 2015.

Friday 10 th		
15.45h - 17.00h		THEORY AND MODELLING (II)
15:45h - 16:00h	Regular	<i>Graphene on an optical waveguide - comparison of simulation approaches</i> J. Čtyroký, P. Kwiecien, J. Petráček, V. Kuzmiak, I. Richter
16:00h - 16:15h	Regular	<i>Unidirectional vectorial eigenmode propagation for multiscale tapered waveguides in 3D</i> L. Ebers, M. Hammer, J. Philipp Höpker, T. Bartley, J. Förstner
16:15h - 16:30h	Regular	<i>Modeling gain in Er³⁺/Yb³⁺ co-doped integrated dual-core waveguides</i> D. Benedicto, A. Días, J. A. Vallés, J. C. Martín, J. Solís
16:30h - 16:45h	Regular	<i>Design Strategy for a Compact Broadband Directional Coupler Using Adiabatically Tapered Waveguides</i> N. Dhingra, E. K. Sharma
16:45h - 17:00h	Regular	<i>Modal Simulation of a Three Lobes Plastic Optical Fiber Bending Sensor</i> D. Sartiano, D. Perez Galacho, F. Berghmans, T. Geernaert, S. Sales

Graphene on an optical waveguide: comparison of simulation approaches

Jiří Čtyrský^{1*}, Pavel Kwiecien², Jiří Petráček³, Vladimír Kuzmiak¹, Ivan Richter²

¹CAS, Institute of Photonics and Electronics, Prague, Czech Republic,

²Faculty of Nuclear Sciences and Physical Engineering, Department of Physical Engineering, Czech Technical University in Prague, Czech Republic

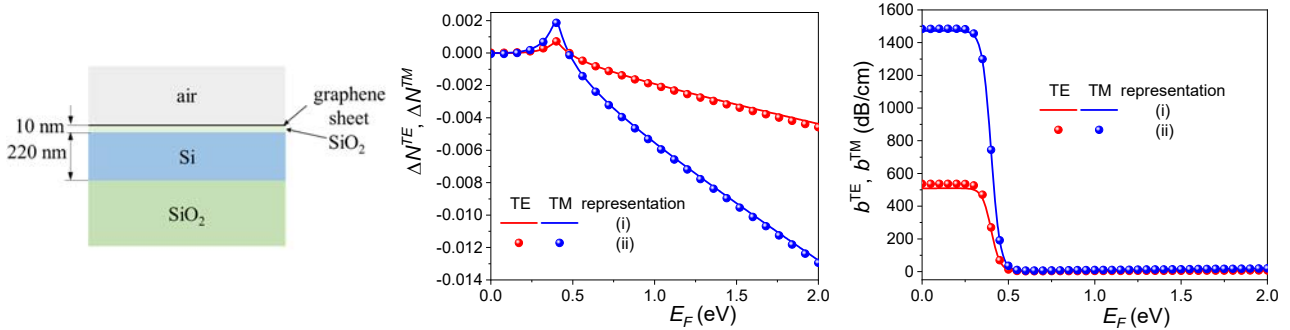
³Faculty of Mechanical Engineering, Brno University of Technology, Brno, Czech Republic

*ctyrosky@ufe.cz

Unusual properties of novel two-dimensional materials like graphene have revolutionized many branches of science and technology. Adequate numerical simulations of photonic devices containing graphene layers requires new approaches or modified methods. In this paper we present comparison of results obtained with two representations of a graphene layer: (i) infinitely thin sheet with a finite surface complex conductivity, and (ii) thin (0.34 nm “thick”) layer of a finite thickness exhibiting uniaxially anisotropic complex permittivity. For both cases, numerical solutions of rigorous dispersion equations were compared to each other and also with the results obtained with commercial as well as proprietary software packets. Both approaches were found to provide comparable results.

Simulation task and results

The surface conductivity of graphene depends on the frequency (wavelength) of the optical field, on the position of the Fermi level in the band diagram of the graphene layer, and on the ambient temperature. To ensure that the results of different simulation approaches are mutually comparable, the same approximate analytical formula for the surface conductivity [1] was used in all simulations. The simulation task was inspired by the structure of a Mach-Zehnder modulator [2] and simplified to a planar waveguide geometry (left figure) that can be described by an analytical dispersion relation.



Waveguide structure.

Calculated change of the effective refractive index and attenuation due to the presence of graphene layer

In the right two graphs we show the change of the real part of the effective refractive index ΔN and attenuation of both TE and TM modes as a function of the Fermi level in the graphene sheet, calculated with representations (i) and (ii) of a graphene layer. Their good agreement indicates that both representations are applicable for the design of photonic devices with graphene layers.

References

- [1] Y.-C. Chang, C.-H. Liu, Z. Zhong, and T. B. Norris, "Extracting the complex optical conductivity of mono- and bilayer Graphene by ellipsometry," *Appl. Phys. Lett.*, vol. 104, no. 26, p. 261909, 2014.
- [2] V. Sorianello, M. Midrio, and M. Romagnoli, "Design optimization of single and double layer graphene phase modulators in SOI," *Optics Express*, vol. 23, no. 5, pp. 6480-6490, 2015.

Unidirectional vectorial eigenmode propagation for multiscale tapered waveguides in 3D

Lena Ebers¹, Manfred Hammer¹, Jan Philipp Höpker², Tim Bartley², Jens Förstner¹

¹ Theoretical Electrical Engineering, Paderborn University, Paderborn, Germany

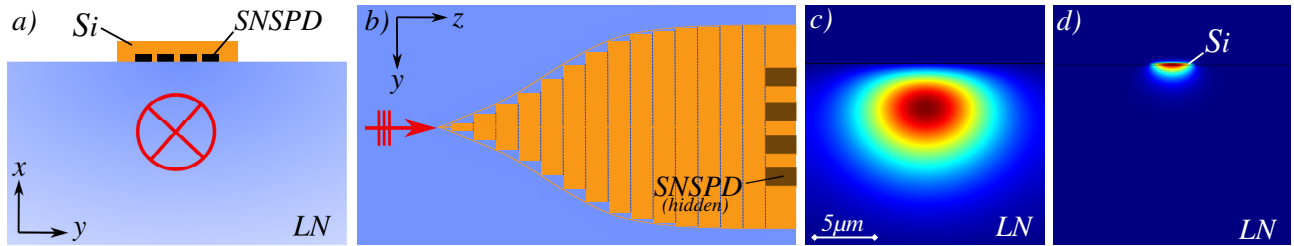
² Applied Physics, Paderborn University, Paderborn, Germany

lana.ebers@uni-paderborn.de

A fast and efficient method to calculate the light propagation along multiscale 3D tapered waveguides is discussed. Vectorial eigenmodes calculated with Comsol Multiphysics constitute the basis for our hybrid numerical/analytical mode matching model.

Superconducting nanowires on lithium niobate waveguides

High efficient and fast single-photon detectors are of huge interest in integrated quantum optics. The combination of Ti-indiffused lithium niobate (LN) waveguides and superconducting nanowire single photon detectors (SNSPDs) enables the observation of quantum effects in an integrated electro-optical platform [1]. Since the power of the incoming mode is concentrated in the LN substrate (Fig.1c), the field overlap with the nanowires, placed on top of the substrate (Fig.1a; without Si-layer), is small and with it the absorption. One possibility to increase the absorption rate is by placing an additional Si-layer on top of the wires to pull up the optical power from the LN mode into the tiny Si-mode (Fig.1d), hence into the region of the detectors. To counteract radiation losses and achieve smooth transitions the Si-layer is of a tapered shape before reaching the wires (Fig.1b). The design of these single-photon detectors require accurate and efficient simulations of these 3D multiscale tapered waveguides.



a) Cross section of the LN waveguide with detectors and Si-layer on top, b) sketch of a tapered waveguide with staircase approximation and view from above, c) guided mode in LN waveguide, d) guided mode in Si-layer.

Finite element modal matching method

We employed a modal matching technique [2], based on a staircase approximation of the tapered shape (Fig.1c), for the calculation of hybrid 3D structures, here transferred to the optical regime with open dielectric waveguides. Back reflections and power transfer through non-guided modes are neglected. Eigenmodes are propagated along the waveguide segments with constant 2D cross sections. Our vectorial 2D mode profiles are calculated with the finite element software Comsol Multiphysics to discretize the different scales of the tiny SNSPDs ($0.16\mu\text{m} \times 0.0035\mu\text{m}$), the small Si-layer ($4\mu\text{m} \times 0.17\mu\text{m}$) and the large LN substrate ($20\mu\text{m} \times 15\mu\text{m}$) precisely. Hence, we call this the finite element modal matching method (FEMMM). By pre-calculating the power overlap products for each combination of cross-sections once, different taper geometries can be simulated within seconds, thus, enabling efficient optimization, e.g for photon detectors with high transmission and low radiation.

References

- [1] J.P. Höpker et al., *Towards integrated superconducting detectors on lithium niobate waveguides*, SPIE Nanoscience + Engineering, San Diego, California, United States, 2017.
- [2] A.D. Olver et al., *Microwave horns and feeds*, IEE Electromagnetic waves series 39, 1994.

Modeling gain in $\text{Er}^{3+}/\text{Yb}^{3+}$ co-doped integrated dual-core waveguides

David Benedicto¹, Antonio Días², Juan A. Vallés^{1,3*}, Juan C. Martín^{1,3}, Javier Solís².

¹ University of Zaragoza, Applied Physics Department, Science Faculty, Zaragoza, Spain

² Laser Processing Group, Institute of Optics, IO-CSIC, Madrid, Spain

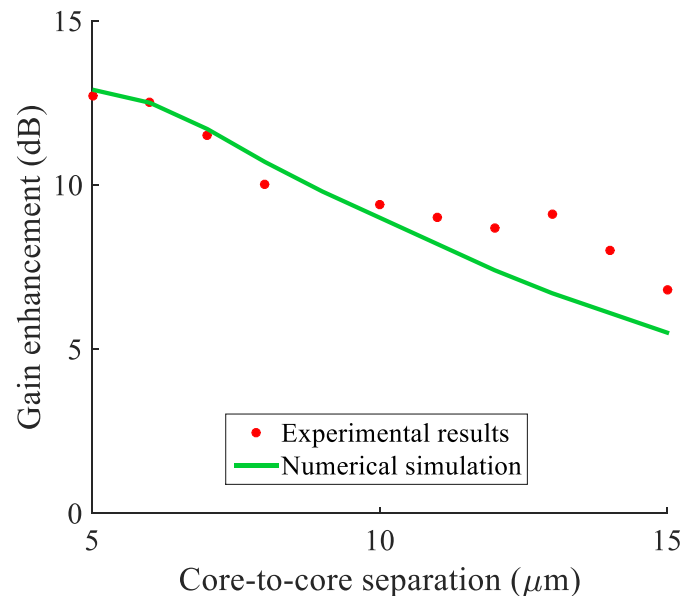
³ Aragon Institute of Engineering Research, Zaragoza, Spain

* juanval@unizar.es

Integrated dual-core waveguides have been fabricated in $\text{Er}^{3+}/\text{Yb}^{3+}$ co-doped phosphate glasses by femtosecond laser writing. A good agreement between numerical results and experimental measurements of the gain enhancement for different core-to-core separation has been achieved.

Irradiation of phosphate glasses with femtosecond laser pulses allows the inscription of 3D integrated waveguides with high refractive index contrast by ion migration mechanisms [1]. Due to the increasing interest on multi-core fibers (MCF) in recent years, active integrated multi-core structures (IMCSs) have been fabricated, measured and simulated.

For the calculations the power propagation equations of the supermodes coupled to the rate equations of the involved active ions were used. Previously, we experimentally determined the necessary characteristic parameters and the supermodes of the integrated dual-core fabricated structure have been characterized and modeled. Significant differences between IMCS and MCF have been taken into account [2]. The accordance between numerical and experimental results is shown in the figure.



Gain enhancement as a function of core-to-core separation with 976-nm bidirectional pump.

References

- [1] T. T. Fernandez, M. Sakakura, S. M. Eaton, B. Sotillo, J. Siegel, J. Solis, Y. Shimotsuma, and K. Miura, "Bespoke photonic devices using ultrafast laser driven ion migration in glasses," *Progress in Materials Science* 94, 68-113 (2018).
- [2] D. Benedicto and J. A. Vallés. "Modeling multicore integrated waveguides in highly doped glass." *Third International Conference on Applications of Optics and Photonics*. Vol. 10453. International Society for Optics and Photonics, 2017.

Design Strategy for a Compact Broadband Directional Coupler Using Adiabatically Tapered Waveguides

Nikhil Dhingra, Enakshi Khular Sharma*

Department of Electronic Science, University of Delhi South Campus, New Delhi – 110021, India

* enakshi@south.du.ac.in

We present the design strategy for a compact and broadband directional coupler based on adiabatic mode evolution in tapered waveguides. The adiabatic taper can be used to split power between the two waveguides within a small length of the coupled section.

Device Design and Optimization

The conventional directional couplers based on evanescent coupling between the individual waveguides are, in general, sensitive to wavelength of operation and fabrication inaccuracies. These limitations can be eliminated by the use of a directional coupler based on adiabatic mode evolution in tapered waveguides [1]. In the coupler configuration shown in Figure 1(a), with $n_1 = 2.847$ and $n_2 = 1.444$, only one supermode is excited (at $\lambda = 1.55 \mu\text{m}$) by the input waveguide and if it propagates adiabatically, the mode will evolve as shown. The final dimensions of the waveguides depend on the splitting ratio required at the output. Based on time dependent perturbation theory [2], it can be shown that for an adiabatic process, the following parameter c_{12} should be kept low (~ 0.02) across the entire length of the taper to minimize the coupling to the second supermode:

$$c_{12} = \frac{a_{12}^+ - a_{12}^-}{\Delta w(\beta_1 - \beta_2)} \left(\frac{dw}{dz} \right)$$

where, a_{12}^+ and a_{12}^- are the excitation coefficient of the second supermode at $(z + \Delta z)/2$ and $(z - \Delta z)/2$ by the first supermode at z and Δw is the corresponding change in the width w . It can be shown that for a linear taper (with constant dw/dz), c_{12} is small around the input and increases rapidly as the waveguides become similar. Hence, an optimal taper with a small slope in the region where the c_{12} is large is required. We have obtained an optimum taper profile (Figure 1(b)) as

$$w(z) = 0.4 + \frac{1}{\alpha} \ln \left(\frac{z}{L} e^{0.1\alpha} - \frac{z}{L} + 1 \right)$$

where, $\alpha = 0.22 \mu\text{m}^{-1}$ for the configuration shown. For adiabaticity (or small c_{12}) across the entire length, for a linear taper, the length L has to be greater than $1000 \mu\text{m}$, whereas for the optimized taper design, a length $L \sim 70 \mu\text{m}$ is adequate as shown in the Figure 1(c).

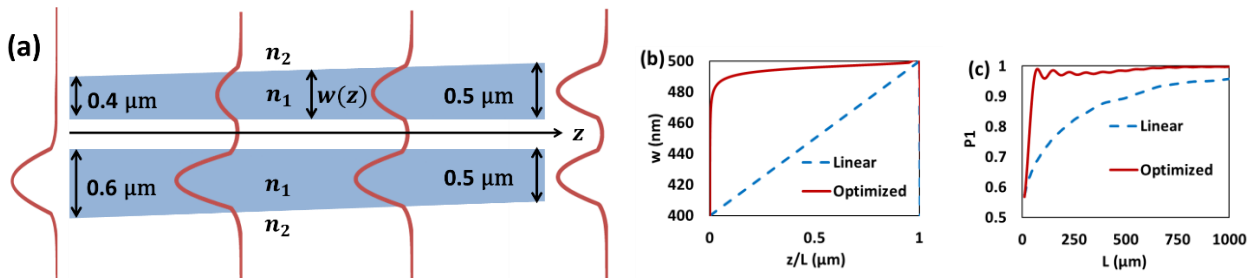


Figure 1. (a) Mode evolution in directional coupler with tapered waveguides (b) taper profiles (c) power in supermode 1 at the end of the taper of length L .

References

- [1] Y. Hung, Z. Li, H. Chung, F. Liang, M. Jung, T. Yen, and S. Tseng, Mode-evolution-based silicon-on-insulator 3 dB coupler using fast quasiadiabatic dynamics, *Opt. Lett.* 44, 815-818 (2019).
- [2] L. I. Schiff (1968), *Quantum Mechanics*, McGraw-Hill, New York.

Modal Simulation of a Three Lobes Plastic Optical Fiber Bending Sensor

Demetrio Sartiano^{1*}, Diego Perez Galacho¹, Francis Berghmans², Thomas Geernaert² and Salvador Sales¹

¹ *Institute of telecommunications and multimedia applications (iTEAM), Universitat Politècnica de València, Camino de Vera, s/n 46022 Valencia SPAIN*

² *Vrije Universiteit Brussel, Pleinlaan 2, 1050 Brussel, Belgium*

* *desar@teleco.upv.es*

A three lobes plastic optical fiber (POF) with polymethylmethacrylate (PMMA) core was fabricated. The aim is to use this POF with non-circular shape as a bending sensor. The mode confinement in the plastic filament that was obtained with an extrusion process was simulated and the effect of bending evaluated.

In this work an optical fiber with non-circular shape was fabricated. Specifically, the fiber consists of a fiber core with three lobes of PMMA surrounded by a polyfluorinated cladding. The filament was directly extruded from plastic pellets, and the trilobal shape was obtained using a customized shaping extrusion die. The three lobes shape of the fiber was conceived to implement a low-cost optical fiber sensor for bending direction and rotation. Sensors based on intensity variation represent one of the first detection schemes used in optical fiber sensors. In terms of operating principle and instrumentation, it may be considered the simplest method. In general, experimental setups include a light source, the optical fiber and a photodetector or an optical spectrum analyzer. The advantages of this measurement method are the ease of implementation, good price/quality ratio and simplicity in signal processing [1]. The bend direction sensing principle is based on the shift of the mode fields that propagate in the three lobes fiber of the PMMA when the plastic filament is bent. As observed in previous calculation and simulation on bent fibers, bending tends to distort the fiber modes, and caused them to shift from the center of curvature [2], considering the variation of the refractive index due to bending along the bending direction (x) with a bending radius R (equation 1).

$$n' = n_{\text{material}} e^{(x/R)} \approx n_{\text{material}} (1 + x/R) \quad (1)$$

The facet of the three lobes fiber was captured with a microscope, processed and imported in Lumerical MODE software. The refractive index of the core and cladding polymers was 1.49 and 1.40 respectively at a wavelength of 645 nm. Simulation of the mode confinement was used to calculate the electric field intensity of the lowest order modes. The modes guided in the straight and bent fiber were computed. It was possible to simulate the mode field in the bent fibers. The electric field intensity for the lowest order modes and three directions of bending was simulated. The results are shown in figure 1.

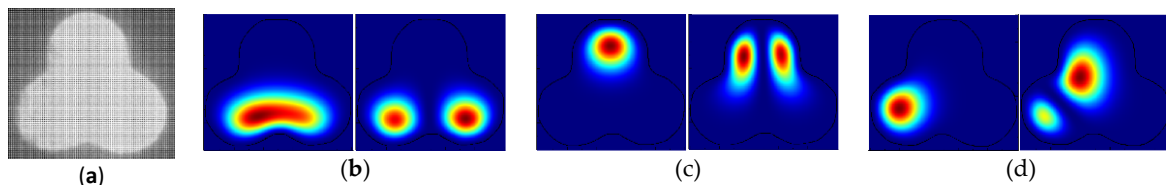


Figure 1. The facet of the three lobes fiber (a). Electric field intensity of the two lowest order modes calculated in the imported three lobes structure for bending with curvature center placed: in the upper side of the fiber (b); in the lower side of the fiber (c); at the right side of the fiber (d).

The results of the simulations will be used to predict the light intensity distribution at the fiber end facet when the sensor is interrogated in transmission.

References

- [1] Kuang, Kevin SC, Wesley J. Cantwell, and Patricia J. Scully. *An evaluation of a novel plastic optical fibre sensor for axial strain and bend measurements*, Measurement Science and Technology 13.10 (2002): 1523.
- [2] Schermer, Ross T., and James H. Cole. *Improved bend loss formula verified for optical fiber by simulation and experiment*, IEEE Journal of Quantum Electronics 43.10 (2007): 899-909.

This work was supported by the European projects blueSPACE (H2020-ICT-2016-2-762055) and FINSESSE (MSCA-ITN-722509), the Spanish project DIMENSION (TEC2017-88029-R), the research Excellence Award Programme GVA (PROMETEO 2017/103) and the Regional Valencian infrastructure project IDI/FEDER/2018. Diego Perez-Galacho acknowledge the support of the Spanish Ministry of Science, Innovation and Universities through the Juan de la Cierva fellowship programme.

Saturday 11 th		
09.30h - 11.00h	GRATINGS	
09:30h - 10:00h	Invited	Subwavelength grating: from basic physics to state-of-the-art devices R. Halir, A. Sánchez-Postigo, J. M. Luque-González, A. Herrero-Bermello, J. Leuermann, A. Ortega-Moñux, J. G. Wangüemert-Pérez, A. V. Velasco, J. de-Oliva-Rubio, J. H. Schmid, P. Cheben, J. Soler Penadés, M. Nedeljkovic, G. Z. Mashanovich, Í. Molina-Fernández
10:00h - 10:15h	Regular	<i>Quasi-total backward reflection with a CRIGF structure under oblique incidence</i> F. Renaud, A. Fehrembach, E. Popov, A. Monmayrant, O. Gauthier-Lafaye
10:15h - 10:30h	Regular	<i>Controlling birefringence in silicon photonics SWG waveguides</i> J. M. Luque-González, A. Herrero-Bermello, A. Ortega-Moñux, Í. Molina-Fernández, A. V. Velasco, P. Cheben, J. H. Schmid, S. Wang, R. Halir
10:30h - 10:45h	Regular	<i>Fast Fourier Factorization: A Powerful Tool for the Modelling of Non-Lamellar Metallic Gratings Compared to the C-Method</i> H. Mohamad, S. Es-Saidi, A. Morand, P. Benech, D. Macias, S. Blaize
10:45h - 11:00h	Regular	Simulation of diffuse scattering due to stochastic disturbances of 1D-gratings M. Heusinger, D. Michaelis, T. Flügel-Paul, U. D. Zeitner

Subwavelength grating: from basic physics to state-of-the-art devices

Robert Halir^{1,2,*}, Alejandro Sánchez-Postigo¹, Jose M. Luque-González¹, Alaine Herrero-Bermello³, Jonas Leuermann², Alejandro Ortega-Moñux¹, Gonzalo Wangüemert-Pérez^{1,2}, Aitor V. Velasco³, Jose de-Oliva-Rubio¹, Jens H. Schmid⁴, Pavel Cheben⁴, Jordi Soler Penadés⁵, Milos Nedeljkovic⁵, Goran Z. Mashanovich⁵, and Íñigo Molina-Fernández^{1,2}

¹ Universidad de Málaga, Dpto. Ingeniería de Comunicaciones, ETSI Telecomunicación, Málaga, Spain

² Bionand Center for Nanomedicine and Biotechnology, Málaga, Spain

³ Instituto de Óptica, Consejo Superior de Investigaciones Científicas, Madrid, Spain

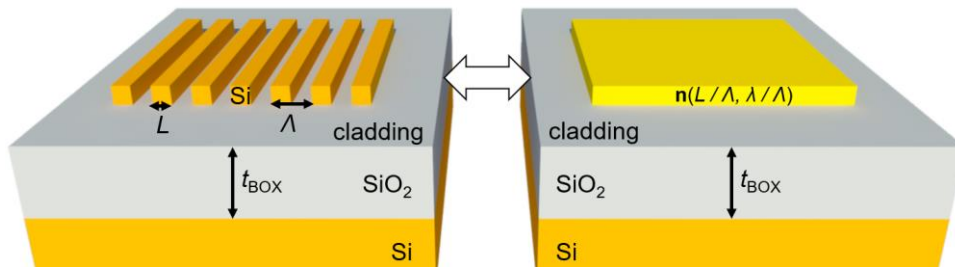
⁴ National Research Council Canada, Ottawa, Ontario, Canada

⁵ Optoelectronics Research Centre, University of Southampton, Southampton, UK

* rhalir@uma.es

Electromagnetic subwavelength structures date back to Hertz's radio wave experiments. With the advent of high-resolution silicon lithography, it has become possible to use such structures to synthesize practical on-chip metamaterials, leading to myriad high-performance integrated devices, which we review here.

A typical silicon subwavelength grating (SWG) consists of an array of silicon strips with a pitch of $\Lambda \sim 250\text{nm}$ for telecom wavelengths around 1550nm . As illustrated in the figure below, for light travelling in the chip plane, such a structure behaves like a homogeneous metamaterial with an equivalent refractive index that depends on the polarization of light, i.e. the metamaterial is anisotropic [1,2]. The refractive index can be engineered by tuning the structural duty-cycle (L/Λ) and its wavelength dependence can be controlled via the wavelength-to-pitch ratio (λ/Λ). This flexibility, combined with straight-forward, single etch step fabrication, has led to the development of a wide variety of high-performance SWG based silicon photonic devices [3]. These include ultra-broadband multi-mode interference couplers, fiber-to-chip couplers with sub-decibel efficiency, and low loss mid-infrared waveguides, the design of which we will review in this contribution.



A silicon slab patterned with a subwavelength pitch ' Λ ' synthesizes an anisotropic metamaterial with an equivalent refractive index tensor dependent on the duty-cycle (L/Λ) and the wavelength-to-pitch ratio (λ/Λ). Here propagation is only considered within the chip plane.

This work was supported by the Ministerio de Economía y Competitividad, Programa Estatal de Investigación, Desarrollo e Innovación Orientada a los Retos de la Sociedad (cofinanciado FEDER), Proyecto TEC2016-80718-R, and the Universidad de Málaga.

References

- [1] H. Hertz, *Ueber Strahlen elektrischer Kraft*, Wiedemanns Ann., vol. 36, p. 769, 1888.
- [2] P. Cheben, et al., *Subwavelength integrated photonics*, Nature, vol. 560, pp. 565–572, 2018
- [3] R. Halir, et al., *Subwavelength-Grating metamaterial structures for silicon photonic devices*, Proc. IEEE, vol. 106, pp. 2144–2157, 2018

Quasi-total backward reflection with a CRIGF structure under oblique incidence

François Renaud^{1&2}, Anne-Laure Fehrembach¹, Evgueni Popov¹, Antoine Monmayrant², Olivier Gauthier-Lafaye²

¹Aix Marseille Univ, CNRS, Centrale Marseille, Institut Fresnel, Marseille, France

²LAAS-CNRS, Université de Toulouse, CNRS, Toulouse, France

*francois.renaud@fresnel.fr

We present new results about the resonant behavior of a cavity resonator integrated grating filter (CRIGF) under oblique incidence. By modifying the structure, the diffracted field distribution can be controlled.

Guided Mode Resonance Filter (GMRF) is a spectral filter composed by a subwavelength grating coupler, etched or deposited on an optical waveguide. Contrary to the well-known multilayer interference filter, it can provide very narrow spectral filtering (Quality factor above 7000), with just a few number of dielectric layers. In a GMRF, an incident wave is coupled, by the grating, to a guided mode of the structure (at the resonance wavelength), causing almost total reflection due to the decoupling of this guided mode. The main issue of this kind of filters is their low angular acceptance, a sharp resonance peak can only be obtained with a collimated beam.

Cavity Resonator Integrated Grating Filter (CRIGF) is a new type of optical filter [1], with narrow bandwidth and high angular acceptance as compared to the Guided Mode Resonance Filter (GMRF). A CRIGF consists of a grating coupler, integrated on a waveguide resonator formed by two Bragg mirrors (as shown in the figure 1). As for the GMRF, an incident wave can be coupled by the grating to a guided mode of the structure. Then, this guided mode is reflected (counter-propagative guided mode) and confined between the two Bragg mirrors, giving a strong and narrow reflection peak in the spectrum, even for very focused incident beam (waist around $5\mu\text{m}$ for $\lambda=850\text{nm}$). Until now, CRIGF have been used under normal incidence only.

We report theoretical modeling of unexpected behavior of the CRIGF under oblique incidence, with four decoupling directions of the two counter-propagative guided modes, instead of the classical outcoupling direction (specular direction in the free space). By adding a gold substrate and a suitable optical buffer layer in the structure, we demonstrate a quasi-total reflection in the counter propagative direction with respect to the incident wave (R_- , see Fig.2).

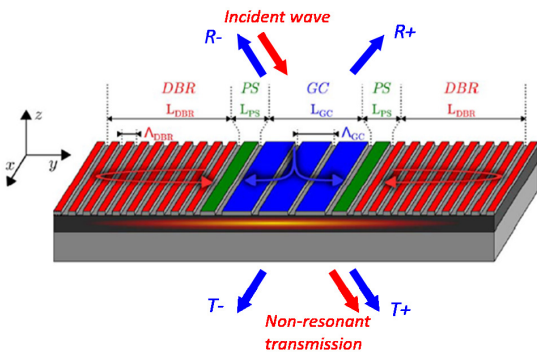


Fig 1: CRIGF under oblique incidence

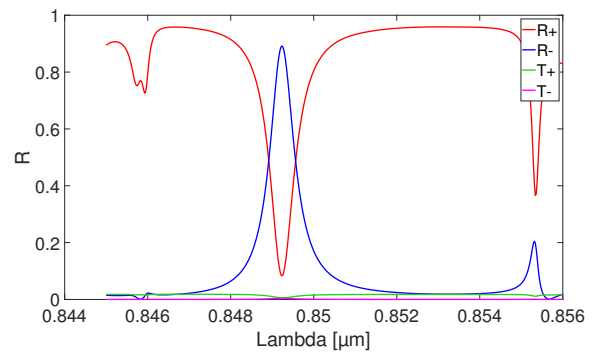


Fig 2: Spectrum of a CRIGF with gold substrate

François Renaud benefit from the PhD funding by the DGA and Aix-Marseille Université

References

- [1] S. Ura, *Proposal of Small-Aperture Guided-Mode Resonance Filter* ICTON 2011, Japan.
- [2] R. Laberdesque, *High-order modes in cavity-resonator-integrated guided-mode resonance filters (CRIGFs)* JOSAA 2015, France.

Controlling birefringence in silicon photonics SWG waveguides

José Manuel Luque-González^{1*}, Alaine Herrero-Bermello², Alejandro Ortega-Moñux¹,
 Íñigo Molina-Fernández^{1,3}, Aitor V. Velasco², Pavel Cheben⁴,

Jens H. Schmid⁴, Shurui Wang⁴ and Robert Halir^{1,3}

¹ Universidad de Málaga, Dpto. Ingeniería de Comunicaciones, ETSI Telecomunicación, Málaga, Spain.

² Institute of Optics, Spanish National Research Council, 28006 Madrid, Spain

³ Bionand Center for Nanomedicine and Biotechnology, Málaga, Spain

⁴ National Research Council Canada, Ottawa, Canada

* jmlg@ic.uma.es

Subwavelength gratings (SWG) work as artificial materials with optical properties dependent on the geometry of the periodic structure. The equivalent refractive index synthesized by an SWG is typically controlled via the pitch and duty cycle of the structure. In this work, we demonstrate the introduction of a new degree of freedom in the canonical SWG geometry: the tilt angle of the silicon segments, providing a precise control over the anisotropy. We propose a simplified anisotropic model that captures the behavior of tilted SWG structures with a much-reduced computational effort compared to rigorous 3D full-vectorial finite difference time domain simulations. Experimental results validate our theoretical calculations, thus confirming the proposed technique to control the birefringence of integrated SWG metamaterial waveguides.

A myriad of high-performance devices SWG based has been reported in the silicon-on-insulator platform [1]. Here we propose to tilt the segment of the SWG structures [Fig. 1(a)], achieving a new degree of freedom. We tune the effective indices of the in-plane (TE) modes, maintaining the out-of-plane (TM) modes virtually unaltered [Fig. 1(b), solid lines]. We justify this behavior by modeling the periodic core as a uniaxial crystal, defined by its permittivity tensor $\epsilon = \text{diag}[(n_{xx}^2, n_{yy}^2, n_{zz}^2)]$. The tilt angle is modeled as a rotation on the axis of the uniaxial crystal, yielding a rotated permittivity tensor: $\tilde{\epsilon} = T^{-1}(\theta)\epsilon T(\theta)$ where T is the rotation matrix in the x-z plane. This model allows us not only to explain the proposed control over the anisotropy but also to quickly and accurately calculate the SWG regime modes. In Fig. 1(b) we compare the 3D-FDTD simulation and the homogenized simulation of the effective index of the modes supported by a tilted SWG structure. A set of measured tilted SWG structures with a tilt angle from 0 to 45 degrees show a variation on the fundamental TE mode effective index of 0.23 refractive index units while the TM mode remain virtually invariant [2].

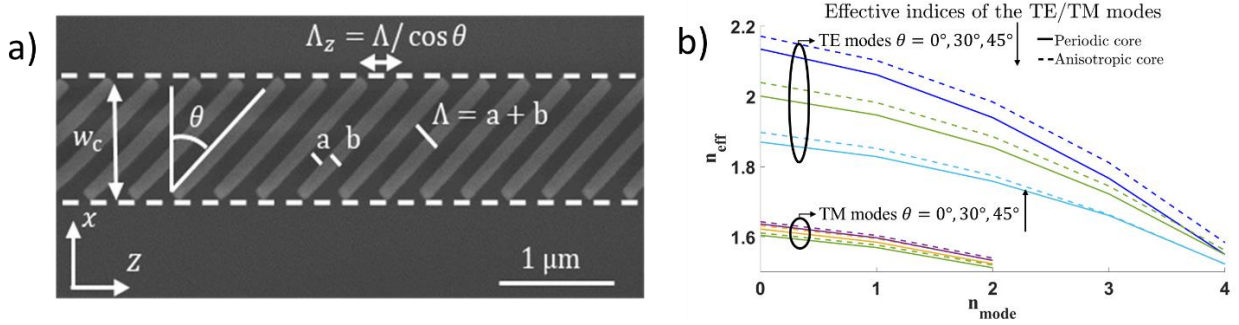


Figure 1. a) Scanning Electron Microscope (SEM) image of a fabricated tilted SWG waveguide. b) Effective indices of all modes on a SWG waveguide, for both polarization, and different tilt angles.

References

- [1] P. Cheben, et al, *Subwavelength integrated photonics*, Nature, Vol. 560, No. 7720, p.565, 2018.
- [2] J. M. Luque-González, et al., *Tilted subwavelength gratings: controlling anisotropy in metamaterial nanophotonic waveguides*, Optics letters, Vol. 43, No. 19, 4691-4694, 2018.

Fast Fourier Factorization: A Powerful Tool for the Modelling of Non-Lamellar Metallic Gratings Compared to the C-Method

Habib Mohamad^{1*}, Soukaina Es-Saidi^{2,3}, Alain Morand¹, Pierre Benech¹, Demetrio Macias², Sylvain Blaize²

¹IMEP-LAHC, Univ. Grenoble Alpes, CNRS, Grenoble INP, 38000 Grenoble, France

²L2n, 12 rue Marie Curie CS 42060 10004 Troyes Cedex, France

³Surys, 22 Avenue de l'Europe, 77607 Bussy-Saint-Georges, France

* habib.mohamad@grenoble-inp.fr

The Rigorous Coupled-Wave Analysis (RCWA) is one of the most popular methods for the modelling of diffraction gratings. It has proven to be particularly effective for Lamellar gratings. However, for non-lamellar metallic gratings, in TM polarization, the Differential Method (DM) or the RCWA need to be associated with the Fast Fourier Factorization (FFF) to provide more accurate solutions.

Numerical Validation and Comparison

For non-lamellar profiles, the RCWA and the DM suffer from very slow convergence. The FFF can then be used to circumvent this problem [1]. In order to appraise the performance of the FFF, we conducted a convergence test comparing the RCWA, the RCWA-FFF, the DM-FFF and the C-Method for the case of a simple sinusoidal Al grating. Then, we studied a triangular Au grating [Fig.1a]. This geometry induces specific resonances at the profile's apexes. It is thus highly recommended to simulate it accurately. However, in this case, two difficulties arise: 1) a profile mixing continuous zones and a discontinuous shape and 2) a metal with a low real part of its complex refractive index. Throughout our numerical simulations, the structure was illuminated with a TM-polarized plane wave. The zero-order reflection R_0 has been evaluated, with respect to the number of harmonics N , with each of the four methods. When the metal is close to the quasi-perfect condition (i.e. $\text{Re}\{n\} \sim 0$), the FFF can diverge in certain cases. Thus, to overcome this problem, some nanometric lossy layers were added [2]. These layers can strongly enhance the convergence of the RCWA-FFF and that of the DM-FFF enabling their stabilities with respect to N , while the C-Method needs a minimum number N higher than 40 to converge to the right value. [Fig.1b]

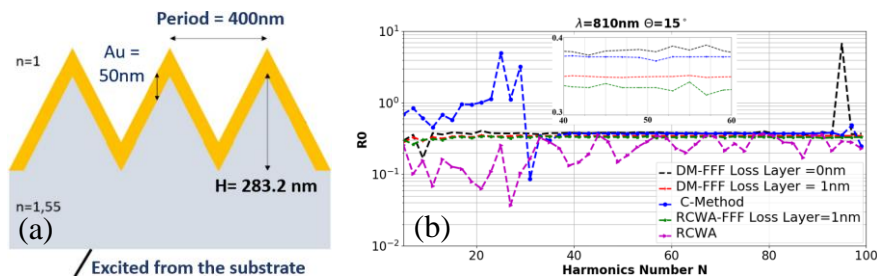


Figure.1 (a) geometry of the triangular Grating (b) R_0 w.r.t N with different thickness of lossy layers.

This work shows, for the first time, the power of the FFF, especially when combined with the RCWA. This result opens the way to simulate non-lamellar gratings faster than the well-known commercial software: MC Grating.

References

- [1] E. Popov & al., J. Opt. Soc. Am. A18, 2886-2894 (2001).
- [2] Yanpeng Mei & al., J. Opt. Soc. Am. A31, 900-906 (2014)

Simulation of diffuse scattering due to stochastic disturbances of 1D-gratings

Martin Heusinger^{1,*}, Dirk Michaelis², Thomas Flügel-Paul², Uwe Detlef Zeitner^{1,2}

¹ *Institut für angewandte Physik, Friedrich-Schiller-Universität Jena, Germany*

² *Fraunhofer-Institut für angewandte Optik und Feinmechanik, Jena, Germany*

*martin.heusinger@uni-jena.de

Simulation of diffuse scattering of optical gratings is a challenging aspect. Due to long range stochastic errors, a numeric evaluation of the problem requires a huge numerical effort. In this paper we present a novel 1D-method that allows to calculate the 2D-diffuse scattering spectra of arbitrarily polarized light on the basis of standard optical simulation tools.

Nowadays, optical gratings are required to fulfill challenging demands. In particular, the stray light performance becomes increasingly critical. The scattered light originates from stochastic disturbances of the grating geometry. So far, the stray light behaviour of gratings is poorly understood and it is therefore of crucial interest to predict the stray light performance of stochastically disturbed gratings. The straight-forward method to calculate the *angle resolved scattering* (ARS) is offered by two-dimensional simulation tools, e.g. the *rigorous coupled wave analysis* (RCWA). Unfortunately, this 2D-approach suffers from computation times that are typically in the range of several days even for small period gratings. However, this restriction can be overcome by just considering the cross-section profile within a 1D-RCWA-simulation (ARS_{1D}). It is shown by analytical considerations within the frame of first Born approximation that the two-dimensionality of the entire problem can be tackled by a multiplication of the 1D-ARS with the *power spectral density* of the disturbance (PSD)

$$ARS_{2D} \cong \left[\frac{n_t}{\lambda} \frac{PSD(k_{s,y} - k_{i,y})}{\sigma^2} \right] \cdot ARS_{1D} = S \cdot ARS_{1D},$$

where σ is the RMS-value of the line displacement, n_t is the refractive index of the transmissive medium and λ is the wavelength. $k_{s/y}$ indicates the y -component of the wavevector of the scattered and incident plane wave, respectively. This relation allows an enormous reduction of the numerical effort, i.e., the computation time can be reduced to only a few seconds. The method can hence be used in order to investigate scattering spectra of various 1D-grating structures. As a verification, Fig. 1 shows conical ARS-simulations of a up-to-date spectrometer grating on the example of *line edge roughness* (LER) as disturbing effect.

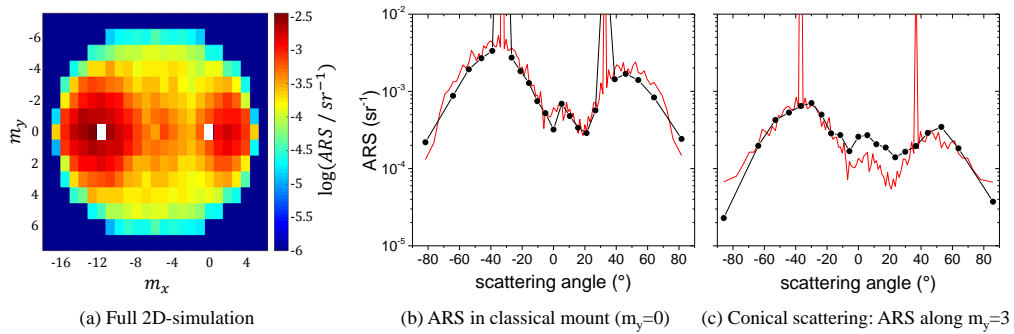


Fig. 1. Simulated scattering spectra within the 1D- and 2D-approach (red line and black dots) for a grating disturbed by LER. 2D-computation: 48 h, 1D-computation: 180 s.

Saturday 11 th		
11:30h - 12:45h	INTEGRATED PHOTONICS	
11:30h - 12:00h	Invited	<i>Nanophotonic circuit components for integrated quantum technology</i> C. Schuck
12:00h - 12:15h	Regular	<i>Design of a subwavelength grating metamaterial GRIN lens</i> J. M. Luque-González, R. Halir, J. de-Oliva-Rubio, J. G. Wangüemert-Pérez, P. Cheben, J. H. Schmid, Í. Molina-Fernández, A. Ortega-Moñux
12:15h - 12:30h	Regular	<i>Simplified modeling of free-carrier based silicon modulators</i> D. Pérez-Galacho, D. Marris-Morini, S. Sales, E. Cassan, C. Baudot, F. Beouf, L. Vivien
12:30h - 12:45h	Regular	<i>Efficient Floquet-Bloch analysis of electrically long quasi-periodic devices</i> A. Hadij-ElHouati, P. Cheben, A. Ortega-Moñux, J. G. Wangüemert-Pérez, R. Halir, J. H. Schmid, Í. Molina-Fernández

Nanophotonic circuit components for integrated quantum technology

Carsten Schuck

University of Münster, Institute of Physics, Münster, Germany

Center for NanoTechnology (CeNTech), Münster, Germany

Center for Soft Nanoscience (SoN), Münster, Germany

* carsten.schuck@uni-muenster.de

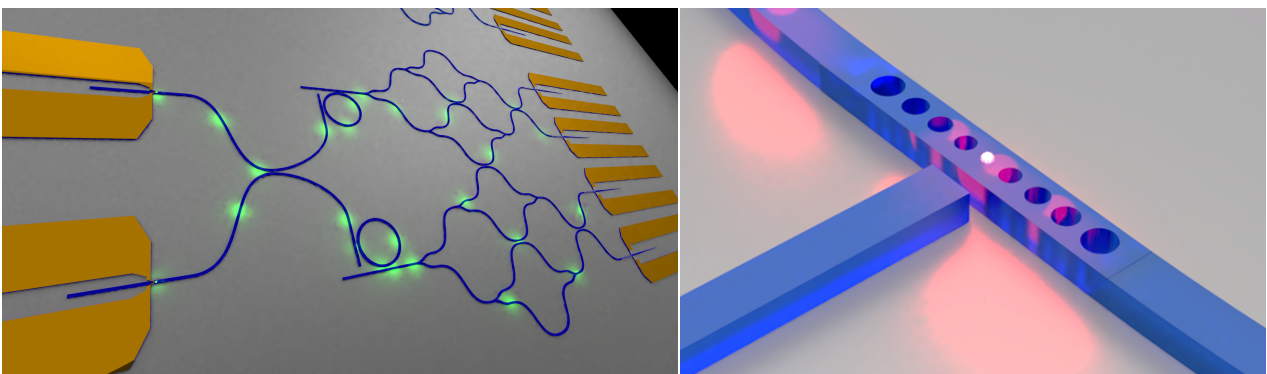
We present progress on realizing highly-efficient and broadband 3D-fiber-to-chip coupling interfaces, inverse design of nanophotonic devices and photonic crystal cavities that allow for strong light-matter interaction as desired for implementing integrated quantum technology with single-photons on silicon chips.

Abstract

Single-photons in nanophotonic circuits on silicon chips hold great promise for future quantum technology [1]. Here we envision a versatile photonic information processor that integrates non-classical light sources, nanophotonic devices and single-photon detectors on a single chip.

The realization of single-photon sources on a nanophotonic chip strongly benefits from efficient interfaces between solid-state quantum emitters and optical waveguides. We achieve this with photonic crystal nanobeam cavities featuring high quality factors and small mode volumes at visible wavelengths. Here we present geometry optimizations based on 3D-FDTD simulations for the SiN-on-insulator material system and experimentally position quantum emitters in close proximity to the defect center of photonic crystal cavities to achieve efficient coupling of single-photons into waveguides supplying a nanophotonic network. As most quantum emitters require optical excitation we further develop broadband interfaces that allow for highly efficient coupling of light between nanophotonic waveguides and optical fibers connected to classical off-chip light sources (lasers). We fabricate near-adiabatic mode converters using a 3D-direct laser writing technique for achieving octave-spanning transmission in the visible wavelength range with low insertion losses.

The manipulation of quantum states encoded in single-photons propagating in a nanophotonic network requires circuit components with a wide range of functionalities. In addition to traditional computer aided design of nanophotonic devices we also pursue inverse design strategies that allow access to a larger solution space. Based on convex optimization techniques we find very compact device designs by employing an objective first approach and performing adjoint sensitivity analysis.



Nanophotonic network schematic for quantum technology applications (left), integrating several circuit components such as resonant light-matter interfaces (right) and other nanophotonic devices.

References

- [1] C. Schuck, X. Guo, L. Fan, X. Ma, M. Poot, H. Tang, *Quantum interference in heterogeneous superconducting-photonic circuits on a silicon chip*, Nature Comm. **7**, 10352, 2016.

Design of a subwavelength grating metamaterial GRIN lens

José Manuel Luque-González^{1*}, Robert Halir¹, José de-Oliva-Rubio¹, J. Gonzalo Wangüemert-Pérez¹, Pavel Cheben², Jens H. Schmid², Íñigo Molina-Fernández¹, Alejandro Ortega-Moñux¹

¹ Universidad de Málaga, Dpto. Ingeniería de Comunicaciones, ETSI Telecomunicación, Málaga, Spain

² National Research Council Canada, Ottawa, Canada

* jmlg@ic.uma.es

In this work we propose a novel integrated graded index (GRIN) lens working as an ultrashort spot-size converter. The device is based on a subwavelength grating (SWG) metamaterial with a constant period in the propagation direction z and an optimized variable duty cycle $DC(x)$. In the design process we take advantage of the inherent anisotropic behavior of SWGs to reduce the size of the lens, achieving an expansion factor $\times 30$ (from $0.5\ \mu\text{m}$ to $15\ \mu\text{m}$) with a device length of $\sim 14\ \mu\text{m}$. Experimental results show measured insertion losses below 1 dB within a wavelength range greater than 130 nm.

Silicon on Insulator (SoI) is nowadays one of the most successful platforms for integrated optics. It provides compatibility with microelectronic CMOS fabrication processes, so it significantly reduces the fabrication cost for massive applications. Since it is a high contrast platform ($\Delta n \sim 2$) the devices are usually very compact and complex functionalities can be achieved using a reduced footprint. One of the main drawbacks of the SoI platform is the limited possibility of using materials different than silicon ($n_{\text{Si}} = 3.476$) and silicon dioxide ($n_{\text{SiO}_2} = 1.444$). Subwavelength grating (SWG) periodic structures overcome this limitation providing a powerful tool to implement artificial metamaterials with optimized properties in terms of refractive index, dispersion and birefringence [1-2].

In this work we propose an integrated GRIN lens based on a z -periodic SWG metamaterial. The duty cycle in the transversal direction $DC(x)$ is optimized to achieve a continuous graded index metamaterial, as can be seen in Fig. 1a). The anisotropic nature of the structure (i.e. $n_{xx} \neq n_{zz}$) must be considered in the design, since it provides a significant reduction of the device length. Figure 1.b) clearly shows how the lens works as a beam expander/collimator. A short adiabatic taper is placed at the input to achieve adaptation between the Si wire and the SWG lens. An expansion factor $\times 30$ (from $0.5\ \mu\text{m}$ to $15\ \mu\text{m}$) is finally achieved with a device as short as $14\ \mu\text{m}$. Minimum feature size constraints MFS $\sim 80\ \text{nm}$ were taken into account to assure e-beam fabricability (see Fig 1.c). Measured insertion losses are below 1 dB within a wavelength range greater than 130 nm.

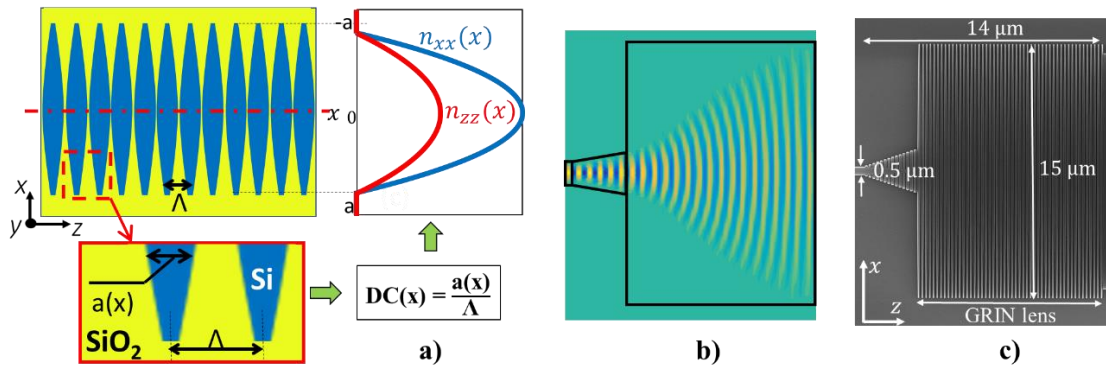


Figure 1. a) Schematic of the z -periodic GRIN SWG lens. b) Simulation of the propagation of the electric field E_x (real part). c) SEM image of the fabricated device.

References

- [1] R. Halir, et al., *Subwavelength-Grating Metamaterial Structures for Silicon Photonic Devices*, Proceedings of the IEEE, No. 99, 1-14, 2018
- [2] P. Cheben, et al, *Subwavelength integrated photonics*, Nature, Vol. 560, No. 7720, p.565, 2018.

Simplified modeling of free-carrier based silicon modulators

Diego Pérez-Galacho^{1,2*}, Delphine Marris-Morini², Salvador Sales¹, Eric Cassan², Charles Baudot³, Frederic Beauf³, Laurent Vivien².

¹ iTEAM Research Institute, Universitat Politècnica de València, Camino de Vera s/n, Valencia 46022, Spain

² Centre de Nanosciences et de Nanotechnologies, CNRS, Univ. Paris-Sud, Université Paris-Saclay, 91120 Palaiseau, France

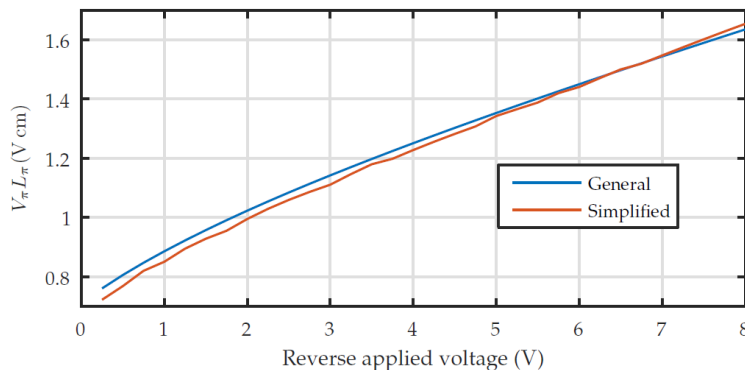
³ ST Microelectronics, 850 rue Jean Monnet, 38920 Crolles, France

* diepega@upv.es

We present the simplified modeling of silicon phase modulators based on the free-carrier plasma dispersion effect. The proposed simplified model enables a substantial reduction in computational effort while maintaining a good accuracy. It is validated against complete 3D-simulations by means of the design of four different modulators.

Modeling of silicon modulators

Silicon photonics is nowadays the reference platform for many applications like sensing and telecommunications. Its natural CMOS compatibility enables the co-integration with current microtechnology circuitry. This feature makes it attractive for next generation photonics based technology, like optical interconnects. Modulators are normally key devices in many applications, like sensors and transmitters. Silicon based modulators are usually based on free-carrier plasma dispersion (FCPD) effect to achieve phase variation [1]. Depending on the targeted application, modulators' specifications change completely. Low loss and high efficiency are required for sensing applications. However, bandwidth is the crucial parameter in telecommunications. Optimizing a modulator for a given application requires many simulation iterations during the design stage. However, simulating a modulator requires a lot of memory and long computation times, in the order of 30 min for a conventional lateral PN junction based modulator. These long simulation times hinder the optimization of the modulator in a reasonable time. In this design stage, a proper modeling of the modulator is of great importance in order to overcome those constraints. In this work, we propose a simplified model for silicon modulators that relax those constraints, without requiring TCAD simulations yet maintaining a good level of accuracy. Using our model, the simulation time of a conventional lateral PN junction based modulator is below 1min, meaning one order of magnitude improvement. A comparison between both models are shown below. Moreover, the relative error of the model compared to a full-physical simulation is below 5%.



Efficiency of a silicon modulator calculated with the proposed model and the general approach.

References

- [1] Reed, Graham T., et al., *Silicon optical modulators*, Nature photonics (2010)

This work was supported by the European project blueSPACE (H2020-ICT-2016-2-762055), the Spanish project DIMENSION (TEC2017-88029-R), the research Excellence Award Programme GVA (PROMETEO 2017/103) and the Regional Valencian infrastructure project IDI/FEDER/2018. Diego Perez-Galacho acknowledge the support of the Spanish Ministry of Science, Innovation and Universities through the Juan de la Cierva fellowship programme.

Efficient Floquet-Bloch analysis of electrically long quasi-periodic devices

A. Hadij-ElHouati^{1,*}, P. Cheben³, A. Ortega-Moñux¹, J. G. Wangüemert-Pérez¹, R. Halir^{1,2}, J. H. Schmid³, Í. Molina-Fernández^{1,2}.

¹ Universidad de Málaga, Dpto. Ingeniería de Comunicaciones, ETSIT, Málaga, Spain

² Bionand Center for Nanomedicine and Biotechnology, Málaga, Spain

³ National Research Council of Canada, Ottawa K1A 0R6, Canada

* abdel@uma.es

In this work we explain a design approach for electrically long quasi-periodic structures based on 3D Floquet-Bloch mode analysis of individual cell elements. This approach obtains results as accurate as 3D FDTD analysis of full device but at a much lower computational effort. For the computation of all the Floquet-Bloch mode parameters a 3D FDTD simulator with periodic boundary conditions and advanced spectral techniques were used. Finally, to verify the proposed technique a sidewall grating (SIGRA) coupler was designed and resulting structure was simulated with 3D FDTD. Good agreement between the Floquet-Bloch approach, requiring computation over one cell only, and the 3D FDTD simulations of the complete structure validate the proposed technique.

Electrically long quasi-periodic devices are very useful in silicon photonics. For these devices to work optimally, the geometry of each one of the hundreds of periods must be designed carefully to meet some predefined design criterium. A 3D vectorial analysis technique must be used to obtain well-performing realistic designs. However, due to the large size of the device, 3D FDTD simulations of the full device require a huge computational resources and a long computation time.

In this work, we propose a computationally efficient design technique that uses 3D Bloch-Floquet analysis for individual element geometry. The only assumption made is that the geometric parameters of the periods change slowly along the propagation direction. A commercial 3D FDTD simulator with periodic boundary conditions and an advanced spectral analysis technique [1] were used to extract the Bloch-Floquet mode parameters (n_{eff} and α) and field profile. Using this technique, we were able to design a distributed Bragg deflector (DBD) [2] in the silicon on insulator platform whose diffracted field profile was engineered to match a predefined Gaussian and is ideally confined in the chip plane (Figure 1.a). The designed device is formed by ~ 80 different element geometries (Figure 1.b). 3D FDTD simulation of the designed device shows that the initial design criteria were met thus reinforcing the correctness and usefulness of the proposed approach

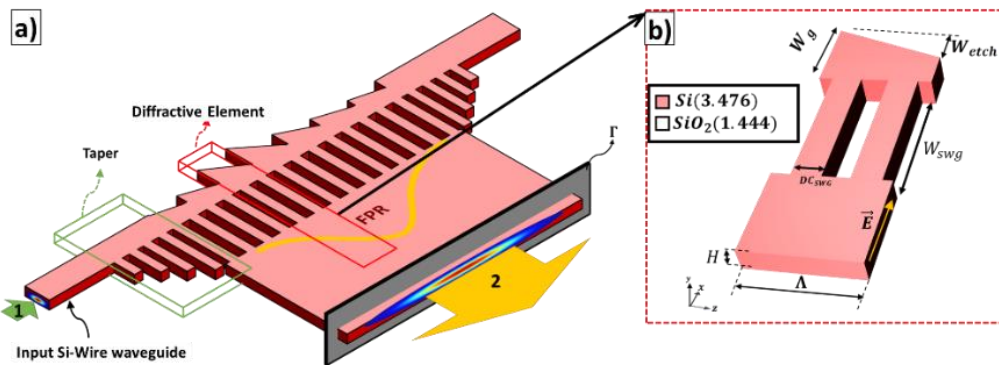


Figure 1. a) Schematic of a DBD formed by variations of a diffractive element geometry (b).

References

- [1] Mandelshtam, V. a. *et al. J. Chem. Phys.* 107, 6756 (1997) DOI:[10.1063/1.475324](https://doi.org/10.1063/1.475324)
- [2] Stoll, H. M. *Appl. Opt.* 17, 2562 (1978) DOI:[10.1364/AO.17.002562](https://doi.org/10.1364/AO.17.002562)

Saturday 11 th		
14.00h - 14.45h		FIBER OPTICS
14:00h - 14:15h	Regular	<i>Splitting of Picosecond Pulses Using Large Mode Area Dispersion Oscillating Fiber at 2.8 μm wavelength</i> M. Rehan, G.Kumar, V. Rastogi
14:15h - 14:30h	Regular	<i>Analysis of Fiber Gratings using a Radial Bidirectional Method</i> R. Kumar, A. Sharma
14:30h - 14:45h	Regular	<i>Optimization of Device Length in Photonic Lanterns using Shortcuts to Adiabaticity</i> S. Sunder, A. Sharma

Splitting of Picosecond Pulses Using Large Mode Area Dispersion Oscillating Fiber at 2.8 μm wavelength

Mohd Rehan, Gyanendra Kumar*, Vipul Rastogi

Indian Institute of Technology Roorkee, Roorkee-247667, Uttarakhand, India

*gyaniitr.mph2017@iitr.ac.in

We propose a large mode area dispersion oscillating fiber and demonstrate propagation of 100 kW peak power picosecond (1.8 ps, 2.8 ps, and 3.5 ps) pulses. We observe splitting of the picosecond pulses at 2.8 μm wavelength. These pulses can be useful for supercontinuum generation and biomedical surgery applications.

The delivery of high-peak-power short duration pulses through few meter length of the fiber finds applications in spectroscopy, communication, remote sensing, and medical fields [1]. Pulse shaping is one of the method to utilize these high peak power pulses more efficiently. Pulse shaping can be achieved by varying dispersion and/or nonlinearity along the length of the fiber [1]. Dispersion decreasing fibers, dispersion compensated fibers, and dispersion oscillating fibers are the examples of these axially varying fibers [1, 2]. In this paper, we propose a large mode area dispersion oscillating fiber (LMADOF). We have studied propagation of 100 kW pulses of durations 1.8 ps, 2.8 ps, and 3.5 ps through 6 m length of the fiber, by solving the nonlinear Schrodinger equation using split-step Fourier method, at 2.8 μm center wavelength. We have observed splitting of the pulse and obtained short duration pulses of peak powers ranging in 100 kW-600 kW at the output end of the fiber as shown in Fig.1. The output high peak power pulses high potential applications in the areas of coherent control, THz electromagnetic wave generation and quasi-phase-matching of high-harmonic generation [1, 3].

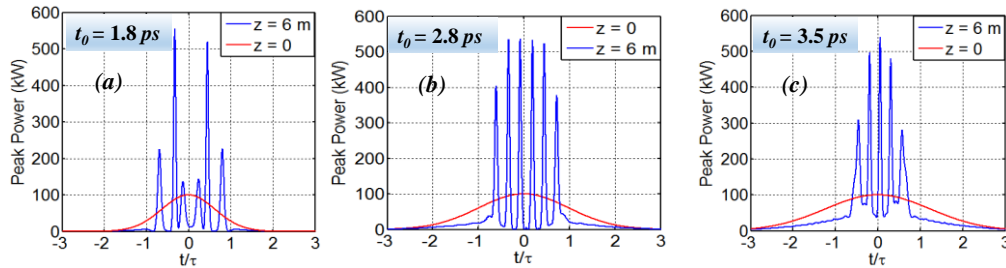


Fig.1. Temporal profiles of input/output pulses for input pulses of 100 kW peak power with duration of (a) 1.8 ps, (b) 2.8 ps, and (c) 3.5 ps. Here z indicates the

Acknowledgement

This work has been partially supported by Department of Science and Technology New Delhi and Russian Science Foundation (DST-RSF) through Indo-Russian project on “Research and development of new optical fibers for applications in modern laser systems.”

References

- [1] G. P. Agarawal, *Nonlinear Fiber Optics*, 5th ed., Academic Press (2013).
- [2] P. Biswas, B. P. Pal, A. Biswas, and S. Ghosh, *Toward Self-Similar Propagation of Optical Pulses in a Dispersion Tailored, Nonlinear, and Segmented Bragg-Fiber at 2.8 μm* . IEEE Photon. J. **9**, 7104412 (2017).
- [3] T. Hornung, R. Meier, and M. Motzkus, *Optimal control of molecular states in a learning loop with a parameterization in frequency and time domain*, Chem. Phys. Lett. **326**, 445-453 (2000).

Analysis of Fiber Gratings using a Radial Bidirectional Method

Ramesh Kumar^{1,2} and Anurag Sharma¹

¹Department of Physics, Indian Institute of Technology Delhi, New Delhi – 110 016 India

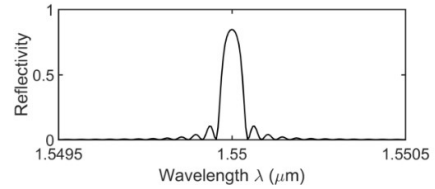
²Department of Physics, Government College for Women, Jind, Haryana, India
rameshpht@gmail.com, asharma@physics.iitd.ac.in

In this paper we propose radial split-step non-paraxial method for the analysis of fiber gratings. The method is bidirectional in nature and is inherently capable of dealing reflections and transmissions in the multiple reflecting surfaces. The method would be useful for modelling fiber grating sensors such as refractive index, strain and temperature sensors.

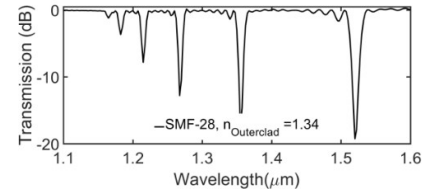
Summary

Fiber gratings - fiber Bragg gratings (FBGs) and long period gratings (LPGs) - are commonly used fiber designs for applications in communication and sensing. An FBG acts as reflector for a particular wavelength which is governed by Bragg's condition whereas LPGs basically couple the core mode into the different cladding modes giving rise to multiple dips in the transmission spectra. The reflection and transmission spectra of FBGs and LPGs is very usually very sensitive to the external changes such as refractive index, strain and the temperature. The coupled mode theory and the transfer matrix method are the commonly employed for the analysis of light propagation in FBGs and LPGs. However, the coupled mode theory is applicable only when the index contrast is small or the perturbation in the core index is weak, and the transfer matrix approach works well with plane wave approximation. Thus, there is a need for a bidirectional method which can deal with the forward and the backward propagation of the waves without any such simplifying approximations.

The spit-step non-paraxial (SSNP) method that we have developed earlier is bidirectional and is inherently capable to deal with the reflections in the multiple reflecting surfaces [1-2]. The split step non-paraxial method in conjunctions with the finite-difference method or the collocation has been used for the analysis of the planar geometries or 2-D structures in Cartesian coordinates. However, fiber gratings are best analyzed in radial coordinates due to their azimuthal symmetry. Here we develop the SSNP the radially symmetric structure using the collocation method with radial basis functions, namely, the Laguerre-Gauss functions. The method is applicable for radially symmetric structures. The effects of the chirping and apodization in the FBGs and LPGs can be investigated very easily. The blazed gratings, however, cannot be analyzed using this method. Modelling of sensors which retail the symmetry can be very easily done using this method. Some examples are shown in the figures and more will be presented.



Reflection spectra of an FBG in SMF-28 fiber for Bragg wavelength 1.55 μm



Transmission spectra of an LPG in SMF-28 fiber with outer clad index 1.34.

Acknowledgement: Anurag Sharma is Class of 66 Chair Professor.

References

- [1] M.S. Shishodia and Anurag Sharma, *Non-iterative bi-directional wave propagation method for treating reflections*, Opt. Commun. **276**, 246-250 (2007).
- [2] D. Bhattacharya and Anurag Sharma, *Simulation of multiple reflecting structures using a non-paraxial bidirectional split-step finite difference method*, J. Lightwave Technol. **31**, 2106-2112 (2013).

Optimization of Device Length in Photonic Lanterns using Shortcuts to Adiabaticity

Sugeet Sunder, Anurag Sharma*

Indian Institute of Technology Delhi, Hauz Khas, New Delhi, India
*sugeet@physics.iitd.ac.in, *asharma@physics.iitd.ac.in*

Adiabatic photonic devices suffer from large device lengths. A Shortcuts to Adiabaticity (STA) protocol is used to optimize the adiabatic taper transition in all-fiber three core photonic lanterns. Adiabaticity was homogenized and the optimized taper transition was 1.8 times shorter than linear adiabatic taper transition.

Summary

A photonic lantern can be realized by adiabatic tapering of a bunch of single mode fibers within a low index capillary, in such a way that N such fibers are tapered together to a final multimode structure which can support N modes [1]. The taper transition in such devices is dependent on satisfying the adiabaticity criterion as outlined in [2]. This condition defines the slowness of the transition, causing such devices to have very large device lengths in order to satisfy the adiabaticity criterion. Shortcuts to adiabaticity (STA) is a class of techniques used widely in quantum control theory to optimize adiabatic transitions [3]. We have optimized the taper transition to achieve shorter device lengths using the ‘fast-quasi adiabatic dynamic protocol outlined in [3]. Three-core photonic lantern having the device dimensions as described in [4] was considered for the analysis. Such devices have three modes, two of which are degenerate.

The adiabaticity criterion mathematically is $|\langle a|\dot{b}\rangle/(\beta_a - \beta_b)| \ll 1$, where the dot denotes derivative with respect to the propagation direction z and β_a & β_b are the propagation constants of the modes $|a\rangle$ and $|b\rangle$, respectively. Along the propagation direction, the device merely tapers, thus leaving a single varying control parameter. We could now calculate the variation of the control parameter with z by imposing the requirement of uniform adiabaticity. Let us consider, $|\langle a|\dot{b}\rangle/(\beta_a - \beta_b)| = c$, where is $c \ll 1$. Now, $|\dot{b}\rangle = \frac{\partial}{\partial z}|b\rangle = \frac{\partial t}{\partial z} \frac{\partial}{\partial t}|b\rangle$, where $t(z)$ is a single control parameter representing the optimized taper transition. Five-point central difference formula is used to compute the required derivative. The optimized device length was found to reduce significantly. More results will be presented including those on non-mode selective photonic lanterns.

Acknowledgement: Anurag Sharma is Class of 66 Chair Professor.

References

- [1] Birks, Timothy A., et al. "The photonic lantern." *Advances in Optics and Photonics* 7.2 (2015)
- [2] Johnson, Steven G., et al. "Adiabatic theorem and continuous coupled-mode theory for efficient taper transitions in photonic crystals." *Physical review E* 66.6 (2002)
- [3] Martínez-Garaot, Sofía, Juan Gonzalo Muga, and Shuo-Yen Tseng. "Shortcuts to adiabaticity in optical waveguides using fast quasiadiabatic dynamics." *Optics express* 25.1 (2017)
- [4] Shen, L., et al "Highly Mode Selective 3-Mode Photonic Lantern through Geometric Optimization," OFC-2018, USA, 2018



XXVII International Workshop on Optical Wave & Waveguide Theory and Numerical Modelling

Málaga, Spain, May 10-11, 2019

<http://www.owtnm2019.com/>